

Morphometric, behavioral, and genomic evidence for a new orangutan species

Authors: Alexander Nater^{1,2,3§*}, Maja P. Mattle-Greminger^{1,2§}, Anton Nurcahyo^{4§}, Matthew G. Nowak^{5,6§}, Marc de Manuel⁷, Tariq Desai⁸, Colin Groves⁴, Marc Pybus⁷, Tugce Bilgin Sonay¹, Christian Roos⁹, Adriano R. Lameira^{10,11}, Serge A. Wich^{12,13}, James Askew¹⁴, Marina Davila-Ross¹⁵, Gabriella Fredriksson^{5,13}, Guillem de Valles⁷, Ferran Casals¹⁶, Javier Prado-Martinez¹⁷, Benoit Goossens^{18,19,20,21}, Ernst J. Verschoor²², Kristin S. Warren²³, Ian Singleton^{5,24}, David A. Marques^{1,25}, Joko Pamungkas^{26,27}, Dyah Perwitasari-Farajallah^{26,28}, Puji Rianti^{28,26,1}, Augustine Tuuga²⁰, Ivo G. Gut^{29,30}, Marta Gut^{29,30}, Pablo Orozco-terWengel¹⁸, Carel P. van Schaik¹, Jaume Bertranpetit^{7,31}, Maria Anisimova^{32,33}, Aylwyn Scally⁸, Tomas Marques-Bonet^{7,29,34}, Erik Meijaard^{4,35*} and Michael Krützen^{1*}

§These authors contributed equally to this work.

*Correspondence to: michael.krutzen@aim.uzh.ch (MK, lead contact), alexander.nater@uzh.ch (AIN), 14 emeijaard@gmail.com (EM),

15 **Affiliations:**

16 ¹Evolutionary Genetics Group, Department of Anthropology, University of Zurich,
17 Winterthurerstrasse 17 190, 8057 Zürich, Switzerland.

18 ²Department of Evolutionary Biology and Environmental Studies, University of Zurich,
19 Winterthurerstrasse 190, 8057 Zürich, Switzerland.

20 ³Lehrstuhl für Zoologie und Evolutionsbiologie, Department of Biology, University of Konstanz,
21 Universitätsstrasse 10, 78457 Konstanz, Germany.

22 ⁴School of Archaeology and Anthropology, Australian National University, Canberra, Australia.

23 ⁵Sumatran Orangutan Conservation Programme (PanEco-YEL), Jalan Wahid Hasyim 51/74, Medan 24
24 20154, Indonesia.

25 ⁶Department of Anthropology, Southern Illinois University, 1000 Faner Drive, Carbondale, IL 62901,
26 USA.

27 ⁷Institut de Biologia Evolutiva (UPF-CSIC), Universitat Pompeu Fabra, Doctor Aiguader 88,
Barcelona 28 08003, Spain.

A NEW SPECIES OF ORANGUTAN

29 ⁸Department of Genetics, University of Cambridge, Downing Street, Cambridge, CB2 3EH, UK.

A NEW SPECIES OF ORANGUTAN

29 ⁹Gene Bank of Primates and Primate Genetics Laboratory, German Primate Center, Leibniz Institute
30 for Primate Research, 37077 Göttingen, Germany.

31 ¹⁰Department of Anthropology, Durham University, Dawson Building, South Road, Durham, DH1
32 3LE, UK.

33 ¹¹School of Psychology & Neuroscience, St. Andrews University, St Mary's Quad, South Street, St.
34 Andrews, Fife, KY16 9JP, Scotland, United Kingdom.

35 ¹²School of Natural Sciences and Psychology, Liverpool John Moores University, James Parsons
36 Building, Byrom Street, L33AF Liverpool, UK.

37 ¹³Institute for Biodiversity and Ecosystem Dynamics, University of Amsterdam, Sciencepark 904,
38 Amsterdam 1098, Netherlands.

39 ¹⁴Department of Biological Sciences, University of Southern California, 3616 Trousdale Parkway, Los
40 Angeles, CA 90089, USA.

41 ¹⁵Department of Psychology, University of Portsmouth, King Henry Building, King Henry 1st Street,
42 Portsmouth, PO1 2DY, UK.

43 ¹⁶Servei de Genòmica, Universitat Pompeu Fabra, Doctor Aiguader 88, Barcelona 08003, Spain.

44 ¹⁷Wellcome Trust Sanger Institute, Wellcome Trust Genome Campus, Hinxton CB10 1SA, UK.

45 ¹⁸School of Biosciences, Cardiff University, Sir Martin Evans Building, Museum Avenue, Cardiff
46 CF10 3AX, UK.

47 ¹⁹Danau Girang Field Centre, c/o Sabah Wildlife Department, Wisma Muis, 88100 Kota Kinabalu,
48 Sabah, Malaysia.

49 ²⁰Sabah Wildlife Department, Wisma Muis, 88100 Kota Kinabalu, Sabah, Malaysia.

50 ²¹Sustainable Places Research Institute, Cardiff University, 33 Park Place, Cardiff CF10 3BA, UK.

51 ²²Department of Virology, Biomedical Primate Research Centre, Lange Kleiweg 161, 2288GJ
52 Rijswijk, The Netherlands.

53 ²³Conservation Medicine Program, College of Veterinary Medicine, Murdoch University, South Street,
54 Murdoch 6150, Australia.

55 ²⁴Foundation for a Sustainable Ecosystem (YEL), Medan, Indonesia.

56 ²⁵Institute of Ecology and Evolution, University of Bern, Baltzerstrasse 6, 3012 Bern, Switzerland.

57 ²⁶Primate Research Center, Bogor Agricultural University, Bogor 16151, Indonesia.

58 ²⁷Faculty of Veterinary Medicine, Bogor Agricultural University, Darmaga Campus, Bogor 16680,
59 Indonesia.

A NEW SPECIES OF ORANGUTAN

60 ²⁸Animal Biosystematics and Ecology Division, Department of Biology, Bogor Agricultural
61 University, Jalan Agatis, Dramaga Campus, Bogor 16680, Indonesia.

62 ²⁹CNAG-CRG, Centre for Genomic Regulation (CRG), Barcelona Institute of Science and Technology
63 (BIST), Baldiri i Reixac 4, Barcelona 08028, Spain.

64 ³⁰Universitat Pompeu Fabra (UPF), Plaça de la Mercè, 10, 08002 Barcelona, Spain.

65 ³¹Leverhulme Centre for Human Evolutionary Studies, Department of Archaeology and Anthropology,
66 University of Cambridge, Cambridge, UK.

67 ³²Institute of Applied Simulations, School of Life Sciences and Facility Management, Zurich
68 University of Applied Sciences ZHAW, Einsiedlerstrasse 31a, 8820 Wädenswil, Switzerland.

69 ³³Swiss Institute of Bioinformatics, Quartier Sorge - Batiment Genopode, 1015 Lausanne, Switzerland.

70 ³⁴Institucio Catalana de Recerca i Estudis Avançats (ICREA), Barcelona 08010, Spain.

71 ³⁵Borneo Futures, Bandar Seri Begawan, Brunei Darussalam.

72 **Summary**

73 Six extant species of non-human great apes are currently recognized: Sumatran and Bornean
74 orangutans, eastern and western gorillas, and chimpanzees and bonobos [1]. However, large gaps
75 remain in our knowledge of fine-scale variation in hominoid morphology, behavior, and genetics, and
76 aspects of great ape taxonomy remain in flux. This is particularly true for orangutans (genus: *Pongo*),
77 the only Asian great apes, and phylogenetically our most distant relatives among extant hominids [1].
78 Designation of Bornean and Sumatran orangutans, *P. pygmaeus* (Linnaeus 1760) and *P. abelii* (Lesson
79 1827), as distinct species occurred in 2001 [1, 2]. Here, we show that an isolated population from
80 Batang Toru, at the southernmost range of extant Sumatran orangutans south of Lake Toba, is distinct
81 from other northern Sumatran and Bornean populations. By comparing cranio-mandibular and dental
82 characters of an orangutan killed in a human-animal conflict to 33 adult male orangutans of similar
83 developmental stage, we found consistent differences between the Batang Toru individual and other
84 extant Ponginae. A second line of evidence provided our analyses of 37 orangutan genomes. Model-
85 based approaches revealed that the deepest split in the evolutionary history of extant orangutans
86 occurred ~3.38 Ma ago between the Batang Toru population and those to the north of Lake Toba,
87 while both currently recognized species separated much later about 674 ka ago. Our combined
88 analyses support a new classification of orangutans into three extant species. The new species, *Pongo*
89 *tapanuliensis*, encompasses the Batang Toru population, of which fewer than 800 individuals survive.

90 **Results and Discussion**

91 Despite decades of field studies [3] our knowledge of variation among orangutans remains limited as
 92 many populations occur in isolated and inaccessible habitats, leaving questions regarding their
 93 evolutionary history and taxonomic classification largely unresolved. In particular, Sumatran
 94 populations south of Lake Toba had long been overlooked, even though a 1939 review of the species’
 95 range mentioned that orangutans had been reported in several forest areas in that region [4]. Based on
 96 diverse sources of evidence, we describe a new orangutan species, *Pongo tapanuliensis*, which
 97 encompasses a geographically and genetically isolated population found in the Batang Toru area at the
 98 southernmost range of extant Sumatran orangutans, south of Lake Toba, Indonesia.

99 *Systematics*

100 Genus *Pongo* Lacépède, 1799

101 *Pongo tapanuliensis* sp. nov. Nurcahyo, Meijaard, Nowak, Fredriksson & Groves Tapanuli

102 Orangutan

103 **Etymology.** The species name refers to three North Sumatran districts (North, Central, and South
 104 Tapanuli) to which *P. tapanuliensis* is endemic.

105 **Holotype.** The complete skeleton of an adult male orangutan that died from wounds sustained by local
 106 villagers in November 2013 near Sugi Tonga, Marancar, Tapanuli (Batang Toru)
 107 Forest Complex (135°54.1’N, 9916’36.5’’E), South Tapanuli District, North
 108 Sumatra, Indonesia. Skull and postcranium are lodged in the Museum Zoologicum Bogoriense,
 109 Indonesia, accession number MZB39182. High-resolution 3D reconstructions of the skull and
 110 mandible are available as supplementary material.

111 **Paratypes.** Adult individuals of *P. tapanuliensis* (P2591-M435788 –
 112 P2591-M435790) photographed by Tim Laman in the Batang Toru Forest
 113 Complex (141°9.1’N, 9859’38.1’’E), North Tapanuli District, North Sumatra, Indonesia. Paratypes are
 114 available from <http://www.morphobank.org> (Login: 2591 / Password: tapanuliorangutan).

115 **Differential diagnosis.** We compared the holotype to a comprehensive comparative data set of 33
 116 adult male orangutans from 10 institutions housing osteological specimens. Unless otherwise stated,
 117 all units are in [mm]. Summary statistics for all measurements are listed in Tables S1–3. *Pongo*
 118 *tapanuliensis* differs from all extant orangutans in the breadth of the upper canine (21.5 vs. <20.86);
 119 the shallow face depth (6.0 vs. >8.4); the narrower interpterygoid distance (at posterior end of
 120 pterygoids 33.8 vs. >43.9; at anterior end of pterygoids, 33.7 vs. >43.0); the shorter tympanic tube
 121 (23.9 vs. >28.4, mostly >30); the shorter temporomandibular joint (22.5 vs. >24.7); the narrower
 122 maxillary incisor row (28.3 vs. >30.1); the narrower distance across the palate at the first molars (62.7

A NEW SPECIES OF ORANGUTAN

123 vs. >65.7); the shorter horizontal length of the mandibular symphysis (49.3 vs. >53.7); the smaller
124 inferior transverse torus (horizontal length from anterior surface of symphysis 31.8 compared to
125 >36.0); and the width of the ascending ramus of the mandible (55.9 vs. >56.3).

126 *Pongo tapanuliensis* differs specifically from *P. abelii* by its deep suborbital fossa, triangular pyriform
127 aperture, and angled facial profile; the longer nuchal surface (70.5 vs. <64.7); the wider rostrum,
128 posterior to the canines (59.9 vs. <59); the narrower orbits (33.8 vs. <34.6); the shorter (29.2 vs.
129 >30.0) and narrower foramen magnum (23.2 vs. >23.3); the narrower bicondylar breadth (120.0 vs.
130 >127.2); the narrower mandibular incisor row (24.4 vs. >28.3); the greater mesio-distal length of the
131 upper canine
132 (19.44 vs. <17.55). The male long call has a higher maximum frequency range of the roar pulse type (>
133 800 Hz vs. <747) with a higher ‘shape’ (>952 Hz/s vs. <934).

134 *Pongo tapanuliensis* differs from *P. pygmaeus* by possessing a nearly straight zygomaxillary suture;
135 the lower orbit (orbit height 33.4 vs. >35.3); the male long call has a longer duration (>111 seconds vs.
136 <90) with a greater number of pulses (>52 pulses vs. <45), and is delivered at a greater rate (>0.82
137 pulses per 20 seconds vs. <0.79).

138 *Pongo tapanuliensis* differs specifically from *Pongo ‘pygmaeus’ palaeosumatrensis* in the smaller size
139 of the first upper molar (mesio-distal length 13.65 vs. >14.0, buccolingual breadth 11.37 vs. >12.10,
140 crown area 155.2 mm² vs. >175.45, Figure S1).

141 **Description.** Craniometrically, the type skull of *P. tapanuliensis* (Figure 1B) is significantly smaller
142 than any skull of comparable developmental stage of other orangutans; it falls outside of the
143 interquartile ranges of *P. abelii* and *P. pygmaeus* for 24 of 39 cranio-mandibular measurements (Table
144 S1). A principal component analysis (PCA) of 26 cranio-mandibular measurements commonly used in
145 primate taxonomic classification [5, 6] shows consistent differences between *P. tapanuliensis* and the
146 two currently recognized species (Figs. 1C and S2).

147 The external morphology of *P. tapanuliensis* is more similar to *P. abelii* in its linear body build and
148 more cinnamon pelage than *P. pygmaeus*. The hair texture of *P. tapanuliensis* is frizzier, contrasting in
149 particular with the long, loose body hair of *P. abelii*. *Pongo tapanuliensis* has a prominent moustache
150 and flat flanges covered in downy hair in dominant males, while flanges of older males resemble more
151 those of Bornean males. Females of *P. tapanuliensis* have beards, unlike *P. pygmaeus*.

152 **Distribution.** *Pongo tapanuliensis* occurs only in a small number of forest fragments in the districts of
153 Central, North, and South Tapanuli, Indonesia (Figure 1A). The total distribution covers
154 approximately 1,000 km², with an estimated population size of fewer than 800 individuals [7]. The
155 current distribution of *P. tapanuliensis* is almost completely restricted to medium elevation hill and
156 submontane forest (~300–1300 m asl) [7–9]. While densities are highest in primary forest, it does

157 occur at lower densities in mixed agroforest at the edge of primary forest areas [10, 11]. Until
158 relatively recently, *P. tapanuliensis* was more widespread to the south and west of the current
159 distribution, although evidence for this is largely anecdotal [12, 13].

160 Other hominoid species and subspecies were previously described using standard univariate and
161 multivariate techniques to quantify morphological character differences. The elevation of bonobos (*P.*
162 *paniscus*) from a subspecies to a species dates back to Coolidge [14] and was based on summary
163 statistics of primarily morphological data from a single female specimen of *P. paniscus*, five available
164 *P. paniscus* skulls, and comparative data of what is now *P. troglodytes*. Groves and colleagues [5] and
165 Shea et al. [15] supported Coolidge's proposal using larger sample sizes and discriminant function
166 analyses. Shea *et al.* [15] remarked that the species designation for *P. paniscus*, which was largely
167 based on morphological comparisons, was ultimately strengthened by genetic, ecological, and
168 behavioral data, as we attempted here for *Pongo tapanuliensis*. For the genus *Gorilla*, Stumpf *et al.*
169 [16] and Groves [17] used cranio-mandibular data from 747 individuals from 19 geographic regions,
170 confirming a classification of the genus into two species (*G. gorilla* and *G. beringei*), as proposed
171 earlier by Groves [1]. Other recent primate species descriptions primarily relied on an inconsistent mix
172 of data on pelage color, ecology, morphology, and/or vocalizations [18-23], with only a few also
173 incorporating genetic analyses [24, 25].

174 Here, we used an integrative approach by corroborating the morphological analysis, behavioral and
175 ecological data with whole-genome data of 37 orangutans with known provenance, covering the entire
176 range of extant orangutans including areas never sampled before (Figure 2A, Table S4). We applied a
177 model-based approach to statistically evaluate competing demographic models, identify independent
178 evolutionary lineages, and infer levels of gene flow and the timing of genetic isolation between
179 lineages. This enabled us to directly compare complex and realistic models of speciation. We refrained
180 from directly comparing genetic differentiation among the three species in the genus *Pongo* with that
181 of other hominoids, as we deem such comparisons problematic in order to evaluate whether *P.*
182 *tapanuliensis* constitutes a new species. This is because estimates of genetic differentiation reflect a
183 combination of divergence time, demographic history, and gene flow, and are also influenced by the
184 employed genetic marker system [26, 27].

185 A PCA (Figure 2B) of genomic diversity highlighted the divergence between individuals from Borneo
186 and Sumatra (PC1), but also separated *P. tapanuliensis* from *P. abelii* (PC2). The same clustering
187 pattern was also found in a model-based analysis of population structure (Figure 2C), and is consistent
188 with an earlier genetic study analyzing a larger number of non-invasively collected samples using
189 microsatellite markers [28]. However, while powerful in detecting extant population structure,
190 population history and speciation cannot be inferred, as they are not suited to distinguish between old
191 divergences with gene flow and cases of recent divergence with isolation [29, 30]. To address this

192 problem and further investigate the timing of population splits and gene flow, we therefore employed
193 different complementary modeling and phylogenetic approaches.

194 We applied an Approximate Bayesian Computation (ABC) approach, which allows to infer and
195 compare arbitrarily complex demographic modes based on the comparison of the observed genomic
196 data to extensive population genetic simulations [31]. Our analyses revealed three deep evolutionary
197 lineages in extant orangutans (Figs. 3A and B). Colonization scenarios in which the earliest split
198 within *Pongo* occurred between the lineages leading to *P. abelii* and *P. tapanuliensis* were much better
199 supported than scenarios in which the earliest split was between Bornean and Sumatran species
200 (models 1 vs. models 2, combined posterior probability: 99.91%, Figure 3A). Of the two best
201 scenarios, a model postulating colonization of both northern Sumatra and Borneo from an ancestral
202 population likely situated south of Lake Toba on Sumatra, had the highest support (model 1a vs. model
203 1b, posterior probability 97.56%, Figure 3A). Our results supported a scenario in which orangutans
204 from mainland Asia first entered Sundaland south of what is now Lake Toba on Sumatra, the most
205 likely entry point based on paleogeographic reconstructions [32]. This ancestral population, of which
206 *P. tapanuliensis* is a direct descendant, then served as a source for the subsequent different
207 colonization events of what is now Borneo, Java and northern Sumatra.

208 We estimated the split time between populations north and south of Lake Toba at ~3.4 Ma (Figure 3B,
209 Table S5). Under our best-fitting model, we found evidence for post-split gene flow across Lake Toba
210 (~0.3–0.9 migrants per generation, Table S5), which is consistent with highly significant signatures of
211 gene flow between *P. abelii* and *P. tapanuliensis* using D-statistics (CK, BT, WA, *Homo sapiens*: $D=$
212 0.2819, $p\text{-value}<0.00001$; WK, BT, LK, *Homo sapiens*: $D= -0.2967$, $p\text{-value}<0.00001$). Such gene
213 flow resulted in higher autosomal affinity of *P. tapanuliensis* to *P. abelii* compared to *P. pygmaeus* in
214 the PCA (Figure 2B), explaining the smaller amount of variance captured by PC2 (separating *P.*
215 *tapanuliensis* from all other populations) compared to PC1 (separating *P. pygmaeus* from the
216 Sumatran populations). The parameter estimates from a Bayesian full-likelihood analysis implemented
217 in the software G-PhoCS were in good agreement with those obtained by the ABC analysis, although
218 the split time between populations north and south of Lake Toba was more recent (~2.27 Ma, 95%-
219 HPD: 2.21– 2.35, Table S5). The G-PhoCS analysis revealed highly asymmetric gene flow between
220 populations north and south of the Toba caldera, with much lower levels of gene flow into the Batang
221 Toru population from the north than vice versa (Table S5).

222 The existence of two deep evolutionary lineages among extant Sumatran orangutans was corroborated
223 by phylogenetic analyses based on whole mitochondrial genomes (Figure 4A), in which the deepest
224 split occurred between populations north of Lake Toba and all other orangutans at ~3.97 Ma (95%-
225 HPD: 2.35–5.57). Sumatran orangutans formed a paraphyletic group, with *P. tapanuliensis* being more
226 closely related to the Bornean lineage from which it diverged ~2.41 Ma (1.26–3.42 Ma). In contrast,

A NEW SPECIES OF ORANGUTAN

227 Bornean populations formed a monophyletic group with a very recent mitochondrial coalescence at
228 ~160 ka (94– 227 ka).

229 Due to strong female philopatry [33], gene flow in orangutans is almost exclusively male-mediated
230 [34].

231 Consistent with these pronounced differences in dispersal behavior, phylogenetic analysis of extensive
232 Y-chromosomal sequencing data revealed a comparatively recent coalescence of Y chromosomes of
233 all extant orangutans ~430 ka (Figure 4B). The single available Y-haplotype from *P. tapanuliensis* was
234 nested within the other Sumatran sequences, pointing at the occurrence of male-mediated gene flow
235 across the Toba divide. Thus, in combination with our modeling results, the sex-specific data
236 highlighted the impact of extraordinarily strong male-biased dispersal in the speciation process of
237 orangutans.

238 Our analyses revealed significant divergence between *P. tapanuliensis* and *P. abelii* (Figs. 3B and 4A),
239 and low levels of male-mediated gene flow (Figs. 3B and 4B), which, however, completely ceased 10–
240 20 ka ago (Figure 3C). Populations north and south of Lake Toba on Sumatra had been in genetic
241 contact for most of the time since their split, but there was a marked reduction in gene flow after ~100
242 ka (Figure 3C), consistent with habitat destruction caused by the Toba supereruption 73 ka ago [35].
243 However, *P. tapanuliensis* and *P. abelii* have been on independent evolutionary trajectories at least
244 since the late
245 Pleistocene/early Holocene, as gene flow between these populations has ceased completely 10–20 ka
246 (Figure 3C) and is now impossible because of habitat loss in areas between the species' ranges [7].

247 Nowadays, most biologists would probably adopt an operational species definition such as: 'a species
248 is a population (or group of populations) with fixed heritable differences from other such populations
249 (or groups of populations)' [36]. With totally allopatric populations, a 'reproductive isolation'
250 criterion, such as is still espoused by adherents of the biological species concept, is not possible [37,
251 38]. Notwithstanding a long-running debate about the role of gene flow during speciation and genetic
252 interpretations of the species concept [39, 40], genomic studies have found evidence for many
253 instances of recent or ongoing gene flow between taxa which are recognized as distinct and well-
254 established species. This includes examples within each of the other three hominid genera. A recent
255 genomic study using comparable methods to ours revealed extensive gene flow between *Gorilla*
256 *gorilla* and *G. beringei* until ~20–30 ka [41]. Similar, albeit older and less extensive, admixture
257 occurred between *Pan troglodytes* and *P. paniscus* [42], and was also reported for *Homo sapiens* and
258 *H. neanderthalensis* [43]. *Pongo tapanuliensis* and *P. abelii* appear to be further examples, showing
259 diagnostic phenotypic and other distinctions that had persisted in the past despite gene flow between
260 them.

261 Due to the challenges involved in collecting suitable specimens for morphological and genomic
262 analyses from critically endangered great apes, our description of *P. tapanuliensis* had to rely on a
263 single skeleton and two individual genomes for our main lines of evidence. When further data will
264 become available, a more detailed picture of the morphological and genomic diversity within this
265 species and of the differences to other *Pongo* species might emerge, which may require further
266 taxonomic revision.

267 However, is not uncommon to describe species based on a single specimen (*e.g.*, [44-46]), and
268 importantly, there were consistent differences among orangutan populations from multiple
269 independent lines of evidence, warranting the designation of a new species with the limited data at
270 hand.

271 With a census size of fewer than 800 individuals [7], *P. tapanuliensis* is the least numerous of all great
272 ape species [47]. Its range is located around 200 km from the closest population of *P. abelii* to the
273 north (Figure 2A). A combination of small population size and geographic isolation is of particular
274 high conservation concern, as it may lead to inbreeding depression [48] and threaten population
275 persistence [49]. Highlighting this, we discovered extensive runs of homozygosity in the genomes of
276 both *P. tapanuliensis* individuals (Figure S3), pointing at the occurrence of recent inbreeding.

277 To ensure long-term survival of *P. tapanuliensis*, conservation measures need to be implemented
278 swiftly. Due to the rugged terrain, external threats have been primarily limited to road construction,
279 illegal clearing of forests, hunting, killings during crop conflict and trade in orangutans [7, 11]. A
280 hydroelectric development has been proposed recently in the area of highest orangutan density, which
281 could impact up to 8% of *P. tapanuliensis*' habitat. This project might lead to further genetic
282 impoverishment and inbreeding, as it would jeopardize chances of maintaining habitat corridors
283 between the western and eastern range (Figure 1A), and smaller nature reserves, all of which maintain
284 small populations of *P. tapanuliensis*.

285 **Author Contributions**

286 Conceived the study and wrote the paper: MPMG, AIN, MK, EM, MGN, CG. Edited the manuscript:
 287 SW, GF, CvS, AS, TMB, DAM, TBS, TD, BG, FC, KSW, EV, POtW, PR, JB, MA, AnN. Carried out
 288 statistical analyses: MPMG, AIN, MGN, AnN, CG, MdM, TD, JA, MDR, AL, MP, JPM, MK, EM,
 289 AS, TMB. Provided samples, and behavioral and ecological data: MGN, MPMG, AnN, AIN, GF, JA,
 290 AL, MDR, BG, EJV, KSW, IS, JP, DPF, PR, WB. Performed sequencing: MPMG, IGG, MG, CR.

291 **Acknowledgments**

292 We thank the following institutions and organizations for supporting our research: Indonesian State
 293 Ministry for Research and Technology, Sabah Wildlife Department, Ministry of Environment and
 294 Forestry of the Republic of Indonesia, Indonesian Institute of Sciences, Leuser International
 295 Foundation, Gunung Leuser National Park, Borneo Orangutan Survival Foundation, Agisoft, NVIDIA,
 296 and the 10 museums where we measured the specimens. This work was financially supported by
 297 University of Zurich (UZH) Forschungskredit grants FK-10 (MPMG), FK-15-103 (AIN), and FK-14-
 298 094 (TBS), Swiss National Science Foundation grant 3100A-116848 (MK, CvS), Leakey Foundation
 299 (MPMG),

300 A.H. Schultz Foundation grants (MK, MPMG), UZH Research Priority Program ‘Evolution in Action’
 301 (MK), the Arcus Foundation (EM), Australian National University (ANU) research fund (AnN), ANU
 302 Vice Chancellor Travel Grant (AnN), Australia Awards Scholarship-DFAT (AnN), ERC Starting
 303 Grant 260372 (TMB), EMBO YIP 2013 (TMB), MINECO BFU2014-55090-P, BFU2015-7116-ERC,
 304 BFU2015-6215-ERCU01, and MH106874 (TMB), Fundacio Zoo Barcelona (TMB), Julius–Klaus
 305 Foundation (MK), MINECO/FEDER BFU2016-77961-P (JB, MP), Gates Cambridge Trust (TD), and
 306 the Department of Anthropology at the University of Zurich. Novel raw sequencing data have been
 307 deposited into the European Nucleotide Archive (ENA; <http://www.ebi.ac.uk/ena>) under study
 308 accession number PRJEB19688.

309 **References**

- 310 1. Groves, C.P. (2001). *Primate taxonomy*, (Washington, D.C. ; London: Smithsonian Institution
 311 Press).
- 312 2. Xu, X., and Arnason, U. (1996). The mitochondrial DNA molecule of Sumatran orangutan
 313 and a molecular proposal for two (Bornean and Sumatran) species of orangutan. *J. Mol. Evol.*
 314 *43*, 431-437.
- 315 3. Wich, S.A., Utami Atmoko, S.S., Mitra Setia, T., and van Schaik, C.P. (2009). *Orangutans:*
 316 *geographic variation in behavioral ecology and conservation*, (Oxford University Press).
- 317 4. Nederlandsch-Indische Vereeniging tot Natuurbescherming (1939). *Natuur in Zuid- en Oost-*
 318 *Borneo. Fauna, flora en natuurbescherming in de Zuider- en Ooster-Afdeeling van Borneo.* In
 319 *3 Jaren Indisch natuur leven. Opstellen over landschappen, dieren en planten, tevens elfde*
 320 *verslag (1936-1938), Nederlandsch-Indische Vereeniging tot Natuurbescherming, ed.*
 321 *(Batavia, Indonesia), pp. 334-411.*

- 322 5. Groves, C.P., Westwood, C., and Shea, B.T. (1992). Unfinished business - Mahalanobis and a
 323 clockwork orang. *J. Hum. Evol.* 22, 327-340.
- 324 6. Groves, C.P. (1986). Systematics of the great apes. In *Comparative primate biology, Vol.1:*
 325 *Systematics, evolution, and anatomy*, D.R. Swindler and J. Erwin, eds. (New York: Alan R.
 326 Liss), pp. 187–217.
- 327 7. Wich, S.A., Singleton, I., Nowak, M.G., Utami Atmoko, S.S., Nisam, G., Arif, S.M., Putra,
 328 R.H., Ardi, R., Fredriksson, G., Usher, G., et al. (2016). Land-cover changes predict steep
 329 declines for the Sumatran orangutan (*Pongo abelii*). *Sci. Adv.* 2, e1500789.
- 330 8. Laumonier, Y., Uryu, Y., Stüwe, M., Budiman, A., Setiabudi, B., and Hadian, O. (2010).
 331 Ecofloristic sectors and deforestation threats in Sumatra: identifying new conservation area
 332 network priorities for ecosystem-based land use planning. *Biodivers. Conserv.* 19, 1153-1174.
- 333 9. Wich, S.A., Usher, G., Peters, H.H., Khakim, M.F.R., Nowak, M.G., and Fredriksson, G.M.
 334 (2014). Preliminary data on the highland Sumatran orangutans (*Pongo abelii*) of Batang Toru.
 335 In *High Altitude Primates*, B.N. Grow, S. Gursky-Doyen and A. Krzton, eds. (New York, NY:
 336 Springer New York), pp. 265-283.
- 337 10. Meijaard, E. (1997). A survey of some forested areas in South and Central Tapanuli, North
 338 Sumatra; new chances for orangutan conservation. (Wageningen: Tropenbos and the Golden
 339 Ark).
- 340 11. Wich, S.A., Fredriksson, G.M., Usher, G., Peters, H.H., Priatna, D., Basalamah, F., Susanto,
 341 W., and Kuhl, H. (2012). Hunting of Sumatran orang-utans and its importance in determining
 342 distribution and density. *Biol. Conserv.* 146, 163-169.
- 343 12. Kramm, W. (1879). Tochtjes in Tapanoeli. *Sumatra-Courant* 20, 1-2.
- 344 13. Miller, G.S. (1903). Mammals collected by Dr. W.L. Abbott on the coast and islands of
 345 northwest Sumatra. *Proceedings US National Museum, Washington* 26, 437-484.
- 346 14. Coolidge, H.J. (1933). *Pan Paniscus*. Pigmy chimpanzee from south of the Congo River. *Am.*
 347 *J. Phys. Anthropol.* 18, 1-59.
- 348 15. Shea, B.T., Leigh, S.R., and Groves, C.P. (1993). Multivariate craniometric variation in
 349 chimpanzees. In *Species, Species Concepts and Primate Evolution*, W.H. Kimbel and L.B.
 350 Martin, eds. (Boston, MA: Springer US), pp. 265-296.
- 351 16. Stumpf, R.M., Polk, J.D., Oates, J.F., Jungers, W.L., Heesy, C.P., Groves, C.P., and Fleagle,
 352 J.G. (2002). Patterns of diversity in gorilla cranial morphology. In *Gorilla biology: a*
 353 *multidisciplinary perspective*, A.B. Taylor and M.L. Goldsmith, eds. (Cambridge: Cambridge
 354 University Press), pp. 35-61.
- 355 17. Groves, C.P. (2002). A history of gorilla taxonomy. In *Gorilla biology: a multidisciplinary*
 356 *perspective*, A.B. Taylor and M.L. Goldsmith, eds. (Cambridge: Cambridge University Press),
 357 pp. 15-34.
- 358 18. Geissmann, T., Lwin, N., Aung, S.S., Aung, T.N., Aung, Z.M., Hla, T.H., Grindley, M., and
 359 Momberg, F. (2011). A new species of snub-nosed monkey, genus *Rhinopithecus*
 360 *MilneEdwards*, 1872 (Primates, Colobinae), from northern Kachin state, northeastern
 361 Myanmar. *Am. J. Primatol.* 73, 96-107.
- 362 19. Jones, T., Ehardt, C.L., Butynski, T.M., Davenport, T.R., Mpunga, N.E., Machaga, S.J., and
 363 De Luca, D.W. (2005). The highland mangabey *Lophocebus kipunji*: a new species of African
 364 monkey. *Science* 308, 1161-1164.
- 365 20. Li, C., Zhao, C., and Fan, P.F. (2015). White-cheeked macaque (*Macaca leucogenys*): a new
 366 macaque species from Medog, southeastern Tibet. *Am. J. Primatol.* 77, 753-766.
- 367 21. Munds, R.A., Nekaris, K.A., and Ford, S.M. (2013). Taxonomy of the Bornean slow loris,
 368 with new species *Nycticebus kayan* (Primates, Lorisidae). *Am. J. Primatol.* 75, 46-56.
- 369 22. Rasoloarison, R.M., Weisrock, D.W., Yoder, A.D., Rakotondravony, D., and Kappeler, P.M.
 370 (2013). Two new species of mouse lemurs (Cheirogaleidae: *Microcebus*) from Eastern
 371 Madagascar. *Int. J. Primatol.* 34, 455-469.
- 372 23. Svensson, M.S., Bersacola, E., Mills, M.S.L., Munds, R.A., Nijman, V., Perkin, A., Masters,
 373 J.C., Couette, S., Nekaris, K.A.I., and Bearder, S.K. (2017). A giant among dwarfs: a new
 374 species of galago (Primates: Galagidae) from Angola. *Am. J. Phys. Anthropol.* 163, 30-43.

- 375 24. Davenport, T.R.B., Stanley, W.T., Sargis, E.J., De Luca, D.W., Mpunga, N.E., Machaga, S.J.,
376 and Olson, L.E. (2006). A new genus of African monkey, *Rungwecebus*: Morphology,
377 ecology, and molecular phylogenetics. *Science* 312, 1378-1381.
- 378 25. Fan, P.F., He, K., Chen, X., Ortiz, A., Zhang, B., Zhao, C., Li, Y.Q., Zhang, H.B., Kimock, C.,
379 Wang, W.Z., et al. (2017). Description of a new species of Hoolock gibbon (Primates:
380 Hylobatidae) based on integrative taxonomy. *Am. J. Primatol.* 79.
- 381 26. Jost, L. (2008). Gst and its relatives do not measure differentiation. *Mol. Ecol.* 17, 4015-4026.
- 382 27. Whitlock, M.C. (2011). G'st and D do not replace Fst. *Mol. Ecol.* 20, 1083-1091.
- 383 28. Nater, A., Arora, N., Greminger, M.P., van Schaik, C.P., Singleton, I., Wich, S.A.,
384 Fredriksson, G., Perwitasari-Farajallah, D., Pamungkas, J., and Krützen, M. (2013). Marked
385 population structure and recent migration in the critically endangered Sumatran orangutan
386 (*Pongo abelii*). *J. Hered.* 104, 2-13.
- 387 29. Nielsen, R., and Wakeley, J. (2001). Distinguishing migration from isolation: a Markov chain
388 Monte Carlo approach. *Genetics* 158, 885-896.
- 389 30. Palsboll, P.J., Berube, M., Aguilar, A., Notarbartolo-Di-Sciara, G., and Nielsen, R. (2004).
390 Discerning between recurrent gene flow and recent divergence under a finite-site mutation
391 model applied to North Atlantic and Mediterranean Sea fin whale (*Balaenoptera physalus*)
392 populations. *Evolution* 58, 670-675.
- 393 31. Beaumont, M.A., Zhang, W.Y., and Balding, D.J. (2002). Approximate Bayesian computation
394 in population genetics. *Genetics* 162, 2025-2035.
- 395 32. Meijaard, E. (2004). Solving mammalian riddles: a reconstruction of the Tertiary and
396 Quaternary distribution of mammals and their palaeoenvironments in island South-East Asia.
397 (Australian National University), p. 2 v.
- 398 33. Arora, N., Van Noordwijk, M.A., Ackermann, C., Willems, E.P., Nater, A., Greminger, M.,
399 Nietlisbach, P., Dunkel, L.P., Utami Atmoko, S.S., Pamungkas, J., et al. (2012).
400 Parentagebased pedigree reconstruction reveals female matrilineal clusters and male-biased
401 dispersal in nongregarious Asian great apes, the Bornean orang-utans (*Pongo pygmaeus*).
402 *Molecular ecology* 21, 3352-3362.
- 403 34. Nater, A., Nietlisbach, P., Arora, N., van Schaik, C.P., van Noordwijk, M.A., Willems, E.P.,
404 Singleton, I., Wich, S.A., Goossens, B., Warren, K.S., et al. (2011). Sex-biased dispersal and
405 volcanic activities shaped phylogeographic patterns of extant orangutans (genus: *Pongo*). *Mol.*
406 *Biol. Evol.* 28, 2275-2288.
- 407 35. Chesner, C.A., Rose, W.I., Deino, A., Drake, R., and Westgate, J.A. (1991). Eruptive history
408 of earth's largest Quaternary caldera (Toba, Indonesia) clarified. *Geology* 19, 200-203.
- 409 36. Groves, C.P., and Grubb, P. (2011). *Ungulate taxonomy*, (Baltimore, Md.: Johns Hopkins
410 University Press).
- 411 37. Coyne, J.A., and Orr, H.A. (2004). *Speciation*, (Sunderland, MA: Sinauer Associates, Inc.).
- 412 38. Mayr, E. (1963). *Animal species and evolution*, (Cambridge: Belknap Press of Harvard
413 University Press).
- 414 39. Arnold, M.L. (2016). *Divergence with Genetic Exchange*, (Oxford, UK: Oxford University
415 Press).
- 416 40. Reznick, D.N., and Ricklefs, R.E. (2009). Darwin's bridge between microevolution and
417 macroevolution. *Nature* 457, 837-842.
- 418 41. Scally, A., Dutheil, J.Y., Hillier, L.W., Jordan, G.E., Goodhead, I., Herrero, J., Hobolth, A.,
419 Lappalainen, T., Mailund, T., Marques-Bonet, T., et al. (2012). Insights into hominid
420 evolution from the gorilla genome sequence. *Nature* 483, 169-175.
- 421 42. de Manuel, M., Kuhlwilm, M., Frandsen, P., Sousa, V.C., Desai, T., Prado-Martinez, J.,
422 Hernandez-Rodriguez, J., Dupanloup, I., Lao, O., Hallast, P., et al. (2016). Chimpanzee
423 genomic diversity reveals ancient admixture with bonobos. *Science* 354, 477.
- 424 43. Kuhlwilm, M., Gronau, I., Hubisz, M.J., de Filippo, C., Prado-Martinez, J., Kircher, M., Fu,
425 Q., Burbano, H.A., Lalueza-Fox, C., de la Rasilla, M., et al. (2016). Ancient gene flow from
426 early modern humans into Eastern Neanderthals. *Nature* 530, 429-433.

- 427 44. Alba, D.M., Almecija, S., DeMiguel, D., Fortuny, J., de los Rios, M.P., Pina, M., Robles, J.M.,
428 and Moya-Sola, S. (2015). Miocene small-bodied ape from Eurasia sheds light on hominoid
429 evolution. *Science* 350.
- 430 45. Stevens, N.J., Seiffert, E.R., O'Connor, P.M., Roberts, E.M., Schmitz, M.D., Krause, C.,
431 Gorscak, E., Ngasala, S., Hieronymus, T.L., and Temu, J. (2013). Palaeontological evidence
432 for an Oligocene divergence between Old World monkeys and apes. *Nature* 497, 611-614.
- 433 46. Zalmout, I.S., Sanders, W.J., MacLatchy, L.M., Gunnell, G.F., Al-Mufarreh, Y.A., Ali, M.A.,
434 Nasser, A.A.H., Al-Masari, A.M., Al-Sobhi, S.A., Nadhra, A.O., et al. (2010). New Oligocene
435 primate from Saudi Arabia and the divergence of apes and Old World monkeys. *Nature* 466,
436 360-U111.
- 437 47. IUCN (2016). IUCN Red List of Threatened Species. Version 2016.2.
- 438 48. Hedrick, P.W., and Kalinowski, S.T. (2000). Inbreeding depression in conservation biology.
439 *Annu. Rev. Ecol. Syst.* 31, 139-162.
- 440 49. Allendorf, F.W., Luikart, G., and Aitken, S.N. (2013). Conservation and the genetics of
441 populations, 2nd Edition, (Hoboken: John Wiley & Sons).
- 442 50. Locke, D.P., Hillier, L.W., Warren, W.C., Worley, K.C., Nazareth, L.V., Muzny, D.M., Yang,
443 S.-P., Wang, Z., Chinwalla, A.T., Minx, P., et al. (2011). Comparative and demographic
444 analysis of orang-utan genomes. *Nature* 469, 529-533.
- 445 51. Prado-Martinez, J., Sudmant, P.H., Kidd, J.M., Li, H., Kelley, J.L., Lorente-Galdos, B.,
446 Veeramah, K.R., Woerner, A.E., O'Connor, T.D., Santpere, G., et al. (2013). Great ape
447 genetic diversity and population history. *Nature* 499, 471-475.
- 448 52. Arora, N., Nater, A., van Schaik, C.P., Willems, E.P., van Noordwijk, M.A., Goossens, B.,
449 Morf, N., Bastian, M., Knott, C., Morrogh-Bernard, H., et al. (2010). Effects of Pleistocene
450 glaciations and rivers on the population structure of Bornean orangutans (*Pongo pygmaeus*).
451 *Proceedings of the National Academy of Sciences* 107, 21376-21381.
- 452 53. Nater, A., Nietlisbach, P., Arora, N., van Schaik, C.P., van Noordwijk, M.A., Willems, E.P.,
453 Singleton, I., Wich, S.A., Goossens, B., Warren, K.S., et al. (2011). Sex-biased dispersal and
454 volcanic activities shaped phylogeographic patterns of extant orangutans (genus: *Pongo*).
455 *Molecular Biology and Evolution* 28, 2275-2288.
- 456 54. van Noordwijk, M.A., Arora, N., Willems, E.P., Dunkel, L.P., Amda, R.N., Mardianah, N.,
457 Ackermann, C., Krützen, M., and van Schaik, C.P. (2012). Female philopatry and its social
458 benefits among Bornean orangutans. *Behavioral Ecology and Sociobiology* 66, 823-834.
- 459 55. Morrogh-Bernard, H.C., Morf, N.V., Chivers, D.J., and Krützen, M. (2011). Dispersal patterns
460 of orang-utans (*Pongo* spp.) in a Bornean peat-swamp forest. *International Journal of*
461 *Primatology* 32, 362-376.
- 462 56. Nietlisbach, P., Arora, N., Nater, A., Goossens, B., Van Schaik, C.P., and Krützen, M. (2012).
463 Heavily male-biased long-distance dispersal of orang-utans (genus: *Pongo*), as revealed by
464 Y-chromosomal and mitochondrial genetic markers. *Molecular ecology* 21, 3173-3186.
- 465 57. Nater, A., Greminger, M.P., Arora, N., van Schaik, C.P., Goossens, B., Singleton, I.,
466 Verschoor, E.J., Warren, K.S., and Krützen, M. (2015). Reconstructing the demographic
467 history of orangutans using Approximate Bayesian Computation. *Molecular Ecology* 24, 310-
468 327.
- 469 58. Drummond, A.J., Suchard, M.A., Xie, D., and Rambaut, A. (2012). Bayesian phylogenetics
470 with BEAUti and the BEAST 1.7. *Molecular biology and evolution* 29, 1969-1973.
- 471 59. Tamura, K., and Nei, M. (1993). Estimation of the number of nucleotide substitutions in the
472 control region of mitochondrial DNA in humans and chimpanzees. *Molecular Biology and*
473 *Evolution* 10, 512-526.
- 474 60. Darriba, D., Taboada, G.L., Doallo, R., and Posada, D. (2012). jModelTest 2: more models,
475 new heuristics and parallel computing. *Nature Methods* 9, 772-772.
- 476 61. Röhrer-Ertl, O. (1988). Research history, nomenclature, and taxonomy of the orang-utan. In
477 *Orang-utan Biology*, J. Schwartz, ed. (Oxford, UK: Oxford University Press), pp. 7-18.
- 478 62. Shapiro, J.S. (1995). Morphometric variation in the orang utan (*Pongo pygmaeus*), with a
479 comparison of inter- and intraspecific variability in the African apes. Volume PhD
480 Dissertation. (Columbia University).

- 481 63. Hooijer, D.A. (1948). Prehistoric teeth of man and of the orang utan from Central Sumatra,
 482 with notes on the fossil orang utan from Java and Southern China. *Zool Meded Rijksmus*
 483 *Leiden* 29, 175 - 183.
- 484 64. Drawhorn, G.M. (1994). The systematics and Paleodemography of fossil Orangutans (Genus
 485 *Pongo*). (University of California).
- 486 65. Harrison, T., Jin, C., Zhang, Y., Wang, Y., and Zhu, M. (2014). Fossil *Pongo* from the Early
 487 Pleistocene Gigantopithecus fauna of Chongzuo, Guangxi, southern China. *Quaternary*
 488 *International* 354, 59-67.
- 489 66. de Vos, J. (1983). The *Pongo* faunas from Java and Sumatra and their significance for
 490 biostratigraphical and paleo-ecological interpretations. *Proceedings of the Koninklijke*
 491 *Akademie van Wetenschappen. Series B* 86, 417-425.
- 492 67. Bacon, A.-M., Westaway, K., Antoine, P.-O., Düringer, P., Blin, A., Demeter, F., Ponche,
 493 J.L., Zhao, J.-X., Barnes, L.M., Sayavonkhamdy, T., et al. (2015). Late Pleistocene
 494 mammalian assemblages of Southeast Asia: New dating, mortality profiles and evolution of
 495 the predator–prey relationships in an environmental context. *Palaeogeography,*
 496 *Palaeoclimatology, Palaeoecology* 422, 101-127.
- 497 68. Louys, J. (2012). Mammal community structure of Sundanese fossil assemblages from the
 498 Late Pleistocene, and a discussion on the ecological effects of the Toba eruption. *Quaternary*
 499 *International* 258, 80-87.
- 500 69. Schwartz, J.H., Vu The, L., Nguyen Lan, C., Le Trung, K., and Tattersall, I. (1995). A review
 501 of the Pleistocene hominoid fauna of the Socialist Republic of Vietnam (excluding
 502 Hylobatidae).
- 503 70. Plavcan, J.M. (1994). Comparison of four simple methods for estimating sexual dimorphism
 504 in fossils. *Am J Phys Anthropol* 94, 465-476.
- 505 71. Greminger, M.P., Stolting, K., Nater, A., Goossens, B., Arora, N., Bruggmann, R., Patrignani,
 506 A., Nussberger, B., Sharma, R., Kraus, R.H., et al. (2014). Generation of SNP datasets for
 507 orangutan population genomics using improved reduced-representation sequencing and direct
 508 comparisons of SNP calling algorithms. *BMC genomics* 15, 16.
- 509 72. Andrews, S. (2012). FastQC. A quality control tool for high throughput sequence data.
- 510 73. Li, H., and Durbin, R. (2009). Fast and accurate short read alignment with Burrows–Wheeler
 511 transform. *Bioinformatics* 25, 1754-1760.
- 512 74. McKenna, A., Hanna, M., Banks, E., Sivachenko, A., Cibulskis, K., Kernysky, A., Garimella,
 513 K., Altshuler, D., Gabriel, S., Daly, M., et al. (2010). The Genome Analysis Toolkit: A
 514 MapReduce framework for analyzing next-generation DNA sequencing data. *Genome*
 515 *Research* 20, 1297-1303.
- 516 75. DePristo, M.A., Banks, E., Poplin, R., Garimella, K.V., Maguire, J.R., Hartl, C., Philippakis,
 517 A.A., del Angel, G., Rivas, M.A., Hanna, M., et al. (2011). A framework for variation
 518 discovery and genotyping using next-generation DNA sequencing data. *Nat Genet* 43, 491-
 519 498.
- 520 76. Derrien, T., Estellé, J., Marco Sola, S., Knowles, D.G., Raineri, E., Guigó, R., and Ribeca, P.
 521 (2012). Fast Computation and Applications of Genome Mappability. *PLoS ONE* 7, e30377.
- 522 77. Auton, A., and McVean, G. (2007). Recombination rate estimation in the presence of hotspots.
 523 *Genome Research* 17, 1219-1227.
- 524 78. Auton, A., Fledel-Alon, A., Pfeifer, S., Venn, O., Segurel, L., Street, T., Leffler, E.M.,
 525 Bowden, R., Aneas, I., Broxholme, J., et al. (2012). A fine-scale chimpanzee genetic map
 526 from population sequencing. *Science* 336, 193-198.
- 527 79. Delaneau, O., Marchini, J., and Zagury, J.F. (2012). A linear complexity phasing method for
 528 thousands of genomes. *Nat Methods* 9, 179-181.
- 529 80. Delaneau, O., Howie, B., Cox, A.J., Zagury, J.F., and Marchini, J. (2013). Haplotype
 530 estimation using sequencing reads. *American Journal of Human Genetics* 93, 687-696.
- 531 81. McQuillan, R., Leutenegger, A.L., Abdel-Rahman, R., Franklin, C.S., Pericic, M., Barac-
 532 Lauc, L., Smolej-Narancic, N., Janicijevic, B., Polasek, O., Tenesa, A., et al. (2008). Runs of
 533 homozygosity in European populations. *American Journal of Human Genetics* 83, 359-372.

- 534 82. Pemberton, Trevor J., Absher, D., Feldman, Marcus W., Myers, Richard M., Rosenberg, Noah
535 A., and Li, Jun Z. (2012). Genomic Patterns of Homozygosity in Worldwide Human
536 Populations. *The American Journal of Human Genetics* 91, 275-292.
- 537 83. Hall, T.A. (1999). BioEdit: a user-friendly biological sequence alignment editor and analysis
538 program for Windows 95/98/NT. In *Nucleic acids symposium series, Volume 41*. pp. 95-98.
- 539 84. Roos, C., Zinner, D., Kubatko, L., Schwarz, C., Yang, M., Meyer, D., Nash, S., Xing, J.,
540 Batzer, M., Brameier, M., et al. (2011). Nuclear versus mitochondrial DNA: evidence for
541 hybridization in colobine monkeys. *BMC Evolutionary Biology* 11, 77.
- 542 85. Thalmann, O., Serre, D., Hofreiter, M., Lukas, D., Eriksson, J., and Vigilant, L. (2005).
543 Nuclear insertions help and hinder inference of the evolutionary history of gorilla mtDNA.
544 *Molecular Ecology* 14, 179-188.
- 545 86. Steiper, M.E., and Young, N.M. (2006). Primate molecular divergence dates. *Molecular*
546 *phylogenetics and evolution* 41, 384-394.
- 547 87. Bellott, D.W., Hughes, J.F., Skaletsky, H., Brown, L.G., Pyntikova, T., Cho, T.-J., Koutseva,
548 N., Zaghul, S., Graves, T., and Rock, S. (2014). Mammalian Y chromosomes retain widely
549 expressed dosage-sensitive regulators. *Nature* 508, 494-499.
- 550 88. Soh, Y.S., Alföldi, J., Pyntikova, T., Brown, L.G., Graves, T., Minx, P.J., Fulton, R.S.,
551 Kremitzki, C., Koutseva, N., and Mueller, J.L. (2014). Sequencing the mouse Y chromosome
552 reveals convergent gene acquisition and amplification on both sex chromosomes. *Cell* 159,
553 800813.
- 554 89. Hughes, J.F., Skaletsky, H., Pyntikova, T., Graves, T.A., van Daalen, S.K., Minx, P.J., Fulton,
555 R.S., McGrath, S.D., Locke, D.P., and Friedman, C. (2010). Chimpanzee and human Y
556 chromosomes are remarkably divergent in structure and gene content. *Nature* 463, 536-539.
- 557 90. Wei, W., Ayub, Q., Chen, Y., McCarthy, S., Hou, Y., Carbone, I., Xue, Y., and Tyler-Smith,
558 C. (2013). A calibrated human Y-chromosomal phylogeny based on resequencing. *Genome*
559 *research* 23, 388-395.
- 560 91. Li, H., Handsaker, B., Wysoker, A., Fennell, T., Ruan, J., Homer, N., Marth, G., Abecasis, G.,
561 Durbin, R., and Subgroup, G.P.D.P. (2009). The Sequence Alignment/Map format and
562 SAMtools. *Bioinformatics* 25, 2078-2079.
- 563 92. Danecek, P., Auton, A., Abecasis, G., Albers, C.A., Banks, E., DePristo, M.A., Handsaker,
564 R.E., Lunter, G., Marth, G.T., Sherry, S.T., et al. (2011). The variant call format and
565 VCFtools. *Bioinformatics* 27, 2156-2158.
- 566 93. Tavaré, S. (1986). Some probabilistic and statistical problems in the analysis of DNA
567 sequences. In *Lectures on Mathematics in the Life Sciences, Volume 17*. pp. 57-86.
- 568 94. Posada, D. (2003). Using MODELTEST and PAUP* to Select a Model of Nucleotide
569 Substitution. In *Current Protocols in Bioinformatics*. (John Wiley & Sons, Inc.).
- 570 95. Drummond, A.J., Ho, S.Y., Phillips, M.J., and Rambaut, A. (2006). Relaxed phylogenetics
571 and dating with confidence. *PLoS biology* 4, e88.
- 572 96. Yang, Z., and Rannala, B. (2006). Bayesian estimation of species divergence times under a
573 molecular clock using multiple fossil calibrations with soft bounds. *Molecular biology and*
574 *evolution* 23, 212-226.
- 575 97. Brunet, M., Guy, F., Pilbeam, D., Mackaye, H.T., Likius, A., Ahounta, D., Beauvilain, A.,
576 Blondel, C., Bocherens, H., and Boissérie, J.-R. (2002). A new hominid from the Upper
577 Miocene of Chad, Central Africa. *Nature* 418, 145-151.
- 578 98. Vignaud, P., Douring, P., Mackaye, H.T., Likius, A., Blondel, C., Boissérie, J.-R., De Bonis,
579 L., Eisenmann, V., Etienne, M.-E., and Geraads, D. (2002). Geology and palaeontology of the
580 Upper Miocene Toros-Menalla hominid locality, Chad. *Nature* 418, 152-155.
- 581 99. Raaum, R.L., Sterner, K.N., Noviello, C.M., Stewart, C.-B., and Disotell, T.R. (2005).
582 Catarrhine primate divergence dates estimated from complete mitochondrial genomes:
583 concordance with fossil and nuclear DNA evidence. *J Hum Evol* 48, 237-257.
- 584 100. Rambaut, A., Suchard, M.A., Xie, D., and Drummond, A.J. (2014). Tracer v1.6.
- 585 101. Rambaut, A. (2012). FigTree version 1.4.

- 586 102. Tamura, K., Stecher, G., Peterson, D., Filipski, A., and Kumar, S. (2013). MEGA6: Molecular
587 Evolutionary Genetics Analysis Version 6.0. *Molecular biology and evolution* *30*, 2725-2729.
- 588 103. Scally, A., and Durbin, R. (2012). Revising the human mutation rate: implications for
589 understanding human evolution. *Nature Reviews Genetics* *13*, 745-753.
- 590 104. Ségurel, L., Wyman, M.J., and Przeworski, M. (2014). Determinants of Mutation Rate
591 Variation in the Human Germline. *Annual Review of Genomics and Human Genetics* *15*, 47-
592 70.
- 593 105. Venn, O., Turner, I., Mathieson, I., de Groot, N., Bontrop, R., and McVean, G. (2014). Strong
594 male bias drives germline mutation in chimpanzees. *Science* *344*, 1272-1275.
- 595 106. Lipson, M., Loh, P.-R., Sankararaman, S., Patterson, N., Berger, B., and Reich, D. (2015).
596 Calibrating the human mutation rate via ancestral recombination density in diploid genomes.
597 *PLoS Genet* *11*, e1005550.
- 598 107. Carbone, L., Alan Harris, R., Gnerre, S., Veeramah, K.R., Lorente-Galdos, B., Huddleston, J.,
599 Meyer, T.J., Herrero, J., Roos, C., Aken, B., et al. (2014). Gibbon genome and the fast
600 karyotype evolution of small apes. *Nature* *513*, 195-201.
- 601 108. Wich, S., De Vries, H., Ancrenaz, M., Perkins, L., Shumaker, R., Suzuki, A., and Van Schaik,
602 C. (2009). Orangutan life history variation. In *Orangutans - Geographic Variation in*
603 *Behavioral Ecology and Conservation* S.A. Wich, S.S. Utami Atmoko, T. Mitra Setia and C.P.
604 van Schaik, eds. (Oxford University Press), pp. 65-75.
- 605 109. Team, R.D.C. (2010). R: a language and environment for statistical computing. (Vienna,
606 Austria: R Foundation for Statistical Computing).
- 607 110. Alexander, D.H., Novembre, J., and Lange, K. (2009). Fast model-based estimation of
608 ancestry in unrelated individuals. *Genome Research* *19*, 1655-1664.
- 609 111. Purcell, S., Neale, B., Todd-Brown, K., Thomas, L., Ferreira, M.A., Bender, D., Maller, J.,
610 Sklar, P., de Bakker, P.I., Daly, M.J., et al. (2007). PLINK: a tool set for whole-genome
611 association and population-based linkage analyses. *Am J Hum Genet* *81*, 559-575.
- 612 112. Schiffels, S., and Durbin, R. (2014). Inferring human population size and separation history
613 from multiple genome sequences. *Nat. Genet.* *46*, 919-925.
- 614 113. Robinson, J.D., Bunnefeld, L., Hearn, J., Stone, G.N., and Hickerson, M.J. (2014). ABC
615 inference of multi-population divergence with admixture from unphased population genomic
616 data. *Mol. Ecol.* *23*, 4458-4471.
- 617 114. Excoffier, L., Smouse, P.E., and Quattro, J.M. (1992). Analysis of molecular variance inferred
618 from metric distances among DNA haplotypes - application to human mitochondrial DNA
619 restriction data. *Genetics* *131*, 479-491.
- 620 115. Hudson, R.R. (2002). Generating samples under a Wright-Fisher neutral model of genetic
621 variation. *Bioinformatics* *18*, 337-338.
- 622 116. Le Cao, K.A., Gonzalez, I., and Dejean, S. (2009). integrOmics: an R package to unravel
623 relationships between two omics datasets. *Bioinformatics* *25*, 2855-2856.
- 624 117. Csillery, K., Francois, O., and Blum, M.G.B. (2012). abc: an R package for approximate
625 Bayesian computation (ABC). *Methods Ecol. Evol.* *3*, 475-479.
- 626 118. Mevik, B.H., and Wehrens, R. (2007). The pls package: principal component and partial least
627 squares regression in R. *J. Stat. Softw.* *18*.
- 628 119. Wegmann, D., Leuenberger, C., and Excoffier, L. (2009). Efficient Approximate Bayesian
629 computation coupled with Markov chain Monte Carlo without likelihood. *Genetics* *182*,
630 12071218.
- 631 120. Leuenberger, C., and Wegmann, D. (2010). Bayesian computation and model selection
632 without likelihoods. *Genetics* *184*, 243-252.
- 633 121. Wegmann, D., Leuenberger, C., Neuenschwander, S., and Excoffier, L. (2010). ABCtoolbox:
634 a versatile toolkit for approximate Bayesian computations. *BMC Bioinformatics* *11*.
- 635 122. Cook, S.R., Gelman, A., and Rubin, D.B. (2006). Validation of software for Bayesian models
636 using posterior quantiles. *J. Comput. Graph. Stat.* *15*, 675-692.
- 637 123. Rice, W.R. (1989). Analyzing tables of statistical tests. *Evolution* *43*, 223-225.

- 638 124. Gronau, I., Hubisz, M.J., Gulko, B., Danko, C.G., and Siepel, A. (2011). Bayesian inference of
639 ancient human demography from individual genome sequences. *Nat. Genet.* 43, 1031-1034.
- 640 125. Baele, G., Lemey, P., Bedford, T., Rambaut, A., Suchard, M.A., and Alekseyenko, A.V.
641 (2012). Improving the accuracy of demographic and molecular clock model comparison while
642 accommodating phylogenetic uncertainty. *Mol Biol Evol* 29, 2157-2167.
- 643 126. Raftery, A.E., Newton, M.A., Satagopan, J.M., and Krivitsky, P.N. (2007). Estimating the
644 integrated likelihood via posterior simulation using the harmonic mean identity. In *Bayesian
645 Statistics*, J.M. Bernardo, M.J. Bayarri and J.O. Berger, eds. (Oxford: Oxford University
646 Press), pp. 1-45.
- 647 127. Röhrer-Ertl, O. (1984). *Orang-utan Studien*, (Neuried, Germany: Hieronymus Verlag).
- 648 128. Röhrer-Ertl, O. (1988). Cranial growth. In *Orang-utan Biology*, J. Schwartz, ed. (Oxford, UK:
649 Oxford University Press), pp. 201-224.
- 650 129. Courtenay, J., Groves, C., and Andrews, P. (1988). Inter- or intra-island variation? An
651 assessment of the differences between Bornean and Sumatran orang-utans. In *Orang-utan
652 biology*, H. Schwartz, ed. (Oxford, England: Oxford University Press), pp. 19-29.
- 653 130. Uchida, A. (1998). Variation in tooth morphology of *Pongo pygmaeus*. *J Hum Evol* 34, 71-79.
- 654 131. Taylor, A.B. (2006). Feeding behavior, diet, and the functional consequences of jaw form in
655 orangutans, with implications for the evolution of *Pongo*. *J Hum Evol* 50, 377-393.
- 656 132. Taylor, A.B. (2009). The functional significance of variation in jaw form in orangutans. In
657 *Orangutans: geographic variation in behavioral ecology and conservation*, S.A. Wich, S.U.
658 Atmoko, T.M. Setia and C.P. van Schaik, eds. (Oxford, UK.: Oxford University Press), pp.
659 1531.
- 660 133. Tukey, J.W. (1977). *Exploratory data analysis*, (London, UK: Addison-Wesley Publishing
661 Company).
- 662 134. Tabachnick, B.G., and Fidell, L.S. (2013). *Using multivariate statistics*, 6th ed, (New York,
663 USA: Pearson).
- 664 135. R Core Development Team (2016). *R: A language and environment for statistical computing*.
665 R Foundation for Statistical Computing. <http://www.R-project.org/>. (Vienna, Austria).
- 666 136. Kaiser, H.F. (1960). The application of electronic computers to factor analysis. *Education and
667 Psychological Measurement* 20, 141-151.
- 668 137. Revelle, W. (2016). *Psych: procedures for personality and psychological research*.
669 <http://CRAN.R-project.org/package=psych> Version =1.6.4, (Evanston, Illinois, USA:
670 Northwestern University).
- 671 138. Davila-Ross, M. (2004). *The long calls of wild male orangutans: A phylogenetic approach*.
672 Volume PhD. (Hannover, Germany: Institut für Zoologie, Tierärztliche Hochschule Hannover).
- 673 139. Davila-Ross, M., and Geissmann, T. (2007). Call diversity of wild male orangutans: a
674 phylogenetic approach. *Am. J. Primatol.* 69, 305-324.
- 675 140. Lameira, A.R., and Wich, S.A. (2008). Orangutan Long Call Degradation and Individuality
676 Over Distance: A Playback Approach. *Int. J. Primatol.* 29, 615-625.
- 677 141. Delgado, R.A., Lameira, A.R., Davila Ross, M., Husson, S.J., Morrogh-Bernard, H.C., and
678 Wich, S.A. (2009). Geographical variation in orangutan long calls. In *Orangutans: Geographic
679 variation in behavioral ecology and conservation*, S.A. Wich, S.S. Utami Atmoko, T. Mitra
680 Setia and C.P. van Schaik, eds. (Oxford, UK: Oxford University Press), pp. 215-224.
- 681 142. Darul Sukma, W.P., Dai, J., Hidayat, A., Yayat, A.H., Sumulyadi, H.Y., Hendra, S., Buurman,
682 P., and Balsem, T. (1990). Explanatory booklet of the land unit and soil map of the Sidikalang
683 sheet (618), Sumatra. (Bogor, Indonesia: Centre for Soil and Agroclimate Research).
- 684 143. Darul Sukma, W.P., Suratman, Hidayat, J.A., and Budhi, P.G. (1990). Explanatory booklet of
685 the land unit and soil map of the Tapaktuan sheet (519), Sumatra, (Bogor, Indonesia: Centre
686 for Soil and Agroclimate Research).
- 687 144. Darul Sukma, W.P., Suratman, Hidayat, J.A., and Budi, P.G. (1990). Explanatory booklet of
688 the land unit and soil map of the Lho'Kruet sheet (420), Sumatra, (Bogor, Indonesia: Centre
689 for Soil and Agroclimate Research).

- 690 145. Darul Sukma, W.P., Verhagen, V., Dai, J., Buurman, P., Balsem, T., Suratman, and Vejre, H.
691 (1990). Explanatory booklet of the land unit and soil map of the Takengon sheet (520),
692 Sumatra, (Bogor, Indonesia: Centre for Soil and Agroclimate Research).
- 693 146. Hidayat, A., Verhagen, A., Darul Sukma, W.P., Buurman, P., Balsem, T., Suratman, and
694 Vejre, H. (1990). Explanatory booklet of the land unit and soil map of the Lhokseumawe (521)
695 and Simpangulim (621) sheets, Sumatra, (Centre for Soil and Agroclimate Research).
- 696 147. Hikmatullah, Wahyunto, Chendy, T.F., Dai, J., and Hidayat, A. (1990). Explanatory booklet of
697 the land unit and soil map of the Langsa (620) sheet, Sumatra, (Bogor, Indonesia: Centre for
698 Soil and Agroclimate Research).
- 699 148. Subardja, D., Djuanda, K., Hadian, Y., Samdan, C.D., Mulyadi, Y., Supriatna, W., and Dai, J.
700 (1990). Explanatory booklet of the land unit and soil map of the Sibolga (617) and
701 Padangsidempuan (717) sheets, Sumatra, (Bogor, Indonesia: Centre for Soil and Agroclimate
702 Research).
- 703 149. Wahyunto, Puksi, D.S., Rochman, A., Wahdini, W., Paidi, Dai, J., Hidayat, A., Buurman, P.,
704 and Balsem, T. (1990). Explanatory booklet of the land unit and soil map of the Medan (619)
705 sheet, Sumatra, (Bogor, Indonesia: Centre for Soil and Agroclimate Research).
- 706 150. Hall, R., van Hattum, M.W.A., and Spakman, W. (2008). Impact of India–Asia collision on
707 SE Asia: The record in Borneo. *Tectonophysics* 451, 366-389.
- 708 151. Hijmans, R.J., Cameron, S.E., Parra, J.L., Jones, P.G., and Jarvis, A. (2005). Very high
709 resolution interpolated climate surfaces for global land areas. *International Journal of*
710 *Climatology* 25, 1965-1978.
- 711 152. Wich, S.A., Singleton, I., Nowak, M.G., Utami Atmoko, S.S., Nisam, G., Arif, S.M., Putra,
712 R.H., Ardi, R., Fredriksson, G., Usher, G., et al. (2016). Land-cover changes predict steep
713 declines for the Sumatran orangutan (*Pongo abelii*). *Science Advances* 2, e1500789.
- 714 153. Wich, S.A., Atmoko, S.U., Setia, T.M., and van Schaik, C. (2009). Orangutans. Geographic
715 variation in behavioral ecology and conservation, (Oxford, UK: Oxford University Press).
- 716 154. Hall, T.A. (1999). BioEdit: a user-friendly biological sequence alignment editor and analysis
717 program for Windows 95/98/NT. *Nucleic acids symposium series* 41, 95-98.
- 718 155. Li, H., Handsaker, B., Wysoker, A., Fennell, T., Ruan, J., Homer, N., Marth, G., Abecasis, G.,
719 and Durbin, R. (2009). The sequence alignment/map format and SAMtools. *Bioinformatics*
720 25, 2078-2079.
- 721 156. Danecek, P., Auton, A., Abecasis, G., Albers, C.A., Banks, E., DePristo, M.A., Handsaker,
722 R.E., Lunter, G., Marth, G.T., Sherry, S.T., et al. (2011). The variant call format and
723 VCFtools. *Bioinformatics* 27, 2156-2158.
- 724 157. Patterson, N., Moorjani, P., Luo, Y., Mallick, S., Rohland, N., Zhan, Y., Genschoreck, T.,
725 Webster, T., and Reich, D. (2012). Ancient admixture in human history. *Genetics* 192,
726 10651093.
- 727 158. Venables, W.N., and Ripley, B.D. (2002). *Modern applied statistics with S*, 4th edition, (New
728 York, USA: Springer).

729 **Figure 1. Morphological evidence supporting a new orangutan species.** A) Current distribution of
 730 *Pongo tapanuliensis* on Sumatra. The holotype locality is marked with a red star. The area shown in
 731 the map is indicated in Figure 2A. B) Holotype skull and mandible of *P. tapanuliensis* from a recently
 732 deceased individual from Batang Toru. See also Figure S1, Tables S1 and S2. C) Violin plots of the
 733 first seven principal components of 26 cranio-mandibular morphological variables of 8 north
 734 Sumatran *P. abelii* and 19 Bornean *P. pygmaeus* individuals of similar developmental state as the
 735 holotype skull (black horizontal lines). See also Figure S2.

736 **Figure 2. Distribution, genomic diversity, and population structure of the genus *Pongo*.** A)
 737 Sampling areas across the current distribution of orangutans. The contour indicates the extent of the
 738 exposed Sunda Shelf during the last glacial maximum. The black rectangle delimits the area shown in
 739 Figure 1A. n = numbers of sequenced individuals. See also Table S4. B) Principal component analysis
 740 of genomic diversity in *Pongo*. Axis labels show the percentages of the total variance explained by the
 741 first two principal components. Colored bars in the insert represent the distribution of nucleotide
 742 diversity in genome-wide 1-Mb windows across sampling areas. C) Bayesian clustering analysis of
 743 population structure using the program ADMIXTURE. Each vertical bar depicts an individual, with
 744 colors representing the inferred ancestry proportions with different assumed numbers of genetic
 745 clusters (K, horizontal sections).

746 **Figure 3. Demographic history and gene flow in *Pongo*.** A) Model selection by Approximate
 747 Bayesian Computation (ABC) of plausible colonization histories of orangutans on Sundaland. The
 748 ABC analyses are based on the comparison of ~3,000 non-coding 2-kb loci randomly distributed
 749 across the genome with corresponding data simulated under the different demographic models. The
 750 numbers in the black boxes indicate the model's posterior probability. NT = Sumatran populations
 751 north of Lake Toba, ST = the Sumatran population of Batang Toru south of Lake Toba, BO = Bornean
 752 populations. B) ABC parameter estimates based on the full demographic model with colonization
 753 pattern inferred in panel A. Numbers in grey rectangles represent point estimates of effective
 754 population size (N_e). Arrows indicate gene flow among populations, numbers above the arrows
 755 represent point estimates of numbers of migrants per generation. See also Table S5. C) Relative cross-
 756 coalescent rate (RCCR) analysis for between-species pairs of phased high-coverage genomes. A
 757 RCCR close to 1 indicates extensive gene flow between species, while a ratio close to 0 indicates
 758 genetic isolation between species pairs. The xaxis shows time scaled in years, assuming a generation
 759 time of 25 years and an autosomal mutation rate of 1.5×10^{-8} per site per generation. See also Figure
 760 S3.

761 **Figure 4. Sex-specific evolutionary history of orangutans.** Bayesian phylogenetic trees for (A)
 762 mitochondrial genomes and (B) Y chromosomes. The mitochondrial tree is rooted with a human and a

A NEW SPECIES OF ORANGUTAN

- 763 central chimpanzee sequence, the Y chromosome tree with a human sequence (not shown). **
- 764 Posterior probability = 1.00. C) Genotype-sharing matrix for mitogenomes (above the diagonal) and Y

A NEW SPECIES OF ORANGUTAN

754 chromosomes (below the diagonal) for all analyzed male orangutans. A value of 1 indicates that two 755 males have identical genotypes at all polymorphic sites; a value of 0 means that they have different 756 genotypes at all variable positions.

756 **CONTACT FOR RESOURCE SHARING**

757 Further information and requests for resources and reagents should be directed to and will be fulfilled
758 by the Lead Contact, Michael Krützen (michael.krutzen@aim.uzh.ch).

759 **EXPERIMENTAL MODEL AND SUBJECT DETAILS**

760 **Sample collection and population assignment for genomic analysis**

761 Our sample set comprised genomes from 37 orangutans, representing the entire geographic range of
762 extant orangutans (Figure 2A). We obtained whole-genome sequencing data for the study individuals
763 from three different sources (Table S4): (i) genomes of 17 orangutans were sequenced for this study.
764 Data for 20 individuals were obtained from (ii) Locke *et al.* [50] (n=10) and (iii) Prado-Martinez *et al.*
765 [51] (n=10). All individuals were wild-born, except for five orangutans which were first-generation
766 offspring of wild-born parents of the same species (Table S4).

767 Population provenance of the previously sequenced orangutans [50, 51] was largely unknown. We
768 identified their most likely natal area based on mtDNA haplotype clustering in a phylogenetic tree
769 together with samples of known geographic provenance. Because of extreme female philopatry in
770 orangutans, mtDNA haplotypes are reliable indicators for the population of origin [33, 52-56]. Using
771 three concatenated mtDNA genes (16S ribosomal DNA, Cytochrome b, and NADH-ubiquinone
772 oxidoreductase chain 3), we constructed a Bayesian tree, including 127 non-invasively sampled wild
773 orangutans from 15 geographic regions representing all known extant orangutan populations [53, 57].
774 Gene sequences of our study individuals were extracted from their complete mitochondrial genome
775 sequences. The phylogenetic tree was built with BEAST v1.8.0. [58], as described in Nater *et al.* [53],
776 applying a TN93+I substitution model [59] as determined by jModelTest v2.1.4. [60].

777 Using the mitochondrial tree, we assigned all previously sequenced orangutans [50, 51] to their most
778 likely population of origin. Our sample assignment revealed incomplete geographic representation of
779 the genus *Pongo* in previous studies. To achieve a more complete representation of extant orangutans,
780 we sequenced genomes of 17 wild-born orangutans mainly from areas with little or no previous
781 sample coverage. Detailed provenance information for these individuals is provided in Table S4.

782 **Samples for morphological analysis**

783 We conducted comparative morphological analyses of 34 adult male orangutans from 10 institutions
784 housing osteological specimens. A single adult male skeleton from the Batang Toru population was
785 available for study, having died from injuries sustained in an orangutan-human conflict situation in
786 November 2013. To account for potential morphological differences related to developmental stage
787 [61,

788 62], our analyses included only males at a similar developmental stage as the Batang Toru specimen,
789 *i.e.*, having a sagittal crest of <10 mm in height. In addition to the single available Batang Toru male,
790 our extant sample comprises specimens from the two currently recognized species, the north Sumatran
791 *Pongo abelii* (n=8) and the Bornean *P. pygmaeus* (n=25).

792 We also evaluated the relationship of the dental material between the Batang Toru specimen and those
793 of the Late Pleistocene fossil material found within the Djamboe, Lida Ajer, and Sibrambang caves
794 near Padang, Sumatra, all of which has been previously described by Hooijer [63]. Some scholars
795 have suggested that the fossil material may represent multiple species [64, 65]. However, Hooijer had
796 more than adequately shown that the variation in dental morphology observed within the three cave
797 assemblages can easily be accommodated within a single species [63]. As only teeth were present in
798 the described cave material, many of which also have gnaw marks, taphonomic processes (*e.g.*,
799 porcupines as accumulating agents) are thought to have largely shaped the cave material [66, 67] and
800 thus may account for the appearance of size differences among the cave samples [64, 65].
801 Furthermore, the similarities in the reconstructed age of the cave material (~128-118 ka or ~80-60 ka
802 [66-68]), and the fact that the presence of more than one large-bodied ape species is an uncommon
803 feature in both fossil and extant Southeast Asian faunal assemblages [69], makes it highly unlikely
804 that multiple large-bodied ape species co-existed within the area at a given time. For purposes of
805 discussion here, we collectively refer to the Padang fossil material as *P. p. palaeosumatrensis*, as
806 described by Hooijer [63].

807 As the comparative fossil sample likely comprises various age-sex classes [63], we divided the fossil
808 sample into two portions above and below the mean for each respective tooth utilized in this study.
809 We considered samples above the mean to represent larger individuals, which we attribute to “males”,
810 and the ones below to being smaller individuals, which we attribute to “females” [70]. We only used
811 the
812 “male” samples in comparison to our extant male comparative orangutan sample.
813

814 **METHOD DETAILS**

815 **Whole-genome sequencing**

816 To obtain sufficient amounts of DNA, we collected blood samples from confiscated orangutans at
817 rehabilitation centres, including the Sumatran Orangutan Conservation Program (SOCP) in Medan,
818 BOS Wanariset Orangutan Reintroduction Project in East Kalimantan, Semongok Wildlife
819 Rehabilitation Centre in Sarawak, and Sepilok Orangutan Rehabilitation Centre in Sabah. We took
820 whole blood samples during routine veterinary examinations and stored in EDTA blood collection
821 tubes at -20°C. The collection and transport of samples were conducted in strict accordance with
822 Indonesian, Malaysian and international regulations. Samples were transferred to Zurich under the

823 Convention on International Trade of Endangered Species in Fauna and Flora (CITES) permit
824 numbers 4872/2010 (Sabah), and 06968/IV/SATS-LN/2005 (Indonesia).

825 We extracted genomic DNA using the Genra Puregene Blood Kit (Qiagen) but modified the protocol
826 for clotted blood as described in Greminger *et al.* [71]. We sequenced individuals on two to three
827 lanes on an Illumina HiSeq 2000 in paired end (2 x 101 bp) mode. Sample PP_5062 was sequenced at
828 the Functional Genomics Center in Zurich (Switzerland), the other individuals at the Centre Nacional
829 d'Anàlisi Genòmica in Barcelona (Spain), as the individuals of Prado-Martinez *et al.* [51]. On
830 average, we generated $\sim 1.1 \times 10^9$ raw Illumina reads per individual.

831 **Read mapping**

832 We followed identical bioinformatical procedures for all 37 study individuals, using the same software
833 versions. We quality-checked raw Illumina sequencing reads with FastQC v0.10.1. [72] and mapped
834 to the orangutan reference genome *ponAbe2* [50] using the Burrows-Wheeler Aligner (BWA-MEM)
835 v0.7.5 [73] in paired-end mode with default read alignment penalty scores. We used Picard v1.101
836 (<http://picard.sourceforge.net/>) to add read groups, convert sequence alignment/map (SAM) files to
837 binary alignment/map (BAM) files, merge BAM files for each individual, and to mark optical and
838 PCR duplicates. We filtered out duplicated reads, bad read mates, reads with mapping quality zero,
839 and reads that mapped ambiguously.

840 We performed local realignment around indels and empirical base quality score recalibration (BQSR)
841 with the Genome Analysis Toolkit (GATK) v3.2.2. [74, 75]. The BQSR process empirically
842 calculates more accurate base quality scores (*i.e.*, Phred-scaled probability of error) than those emitted
843 by the sequencing machines through analysing the covariation among several characteristics of a base
844 (*e.g.*, position within the read, sequencing cycle, previous base, etc.) and its status of matching the
845 reference sequence or not. To account for true sequence variation in the data set, the model requires a
846 database of known polymorphic sites ('known sites') which are skipped over in the recalibration
847 algorithm. Since no suitable set of 'known sites' was available for the complete genus *Pongo*, we
848 preliminary identified confident SNPs from our data. For this, we performed an initial round of SNP
849 calling on unrecalibrated BAM files with the *UnifiedGenotyper* of the GATK. Single nucleotide
850 polymorphisms were called separately for Bornean and Sumatran orangutans in multi-sample mode
851 (*i.e.*, joint analysis of all individuals per island), creating two variant call (VCF) files. In addition, we
852 produced a third VCF file jointly analysing all study individuals in order to capture genus-wide low
853 frequency alleles. We applied the following hard quality filter criteria on all three VCF files: QUAL <
854 50.0 || QD < 2.0 || FS > 60.0 || MQ < 40.0 || HaplotypeScore > 13.0 || MappingQualityRankSum < -12.5 ||
855 ReadPosRankSum < -8.0. Additionally, we calculated the mean and standard deviation of sequencing
856 depth over all samples and filtered all sites with a site-wise coverage more than five standard
857 deviations above the mean. We merged the three hard filtered VCF files and took SNPs as 'known

858 sites' for BQSR with the GATK. The walkers CountReads and DepthOfCoverage of the GATK were
859 used to obtain various mapping statistics for unfiltered and filtered BAM files.

860 Mean effective sequencing depth, estimated from filtered BAM files, varied among individuals
861 ranging from 4.8–12.2x [50] to 13.7–31.1x (this study) [51], with an average depth of 18.4x over all
862 individuals (Tables S4). For the previously sequenced genomes [50, 51], estimated sequence depths
863 were 25–40% lower as the values reported in the two source studies. This difference is explained by
864 the way sequence depth was calculated. Here, we estimated sequence depth on the filtered BAM files
865 where duplicated reads, bad read mates, reads with mapping quality zero, and reads which mapped
866 ambiguously had already been removed. Thus, our sequence coverage estimates correspond to the
867 effective read-depths which are available for SNP discovery and genotyping.

868 **SNP and genotype calling**

869 We produced high quality genotypes for all individuals for each position in the genome, applying the
870 same filtering criteria for SNP and non-polymorphic positions. We identified SNPs and called
871 genotypes in a three-step approach. First, we identified a set of candidate (raw) SNPs among all study
872 individuals. Second, we performed variant quality score recalibration (VQSR) on the candidate SNPs
873 to identify high-confidence SNPs. Third, we called genotypes of all study individuals at these
874 highconfidence SNP positions.

875 Step 1: We used the *HaplotypeCaller* of the GATK in genomic Variant Call Format (gVCF) mode to
876 obtain for each individual in the dataset genotype likelihoods at any site in the reference genome.
877 *HaplotypeCaller* performs local realignment of reads around potential variant sites and is therefore
878 expected to considerably improve SNP calling in difficult-to-align regions of the genome. We then
879 genotyped the resulting gVCF files together on a per-island level, as well as combined for all
880 individuals, using the *Genotype GVCFs* tool of the GATK to obtain three VCF files with candidate
881 SNPs for *P. abelii*, *P. pygmaeus*, and over all *Pongo* samples.

882 Step 2: Of the produced set of candidate SNPs, we identified high-confidence SNPs using the VQSR
883 procedure implemented in the GATK. The principle of the method is to develop an estimate of the
884 relationship between various SNP call annotations (*e.g.*, total depth, mapping quality, strand bias, etc.)
885 and the probability that a SNP is a true genetic variant. The model is determined adaptively based on a
886 set of 'true SNPs' (*i.e.*, known variants) provided as input. Our 'true SNPs' set contained 5,600
887 highconfidence SNPs, which were independently identified by three different variant callers in a
888 previous reduced-representation sequencing project [71]. We ran the *Variant Recalibrator* of the
889 GATK separately for each of the three raw SNP VCFs to produce recalibration files based on the 'true
890 SNPs' and a VQSR training set of SNPs. The VQSR training sets were derived separately for each of
891 the three raw SNP VCF files and contained the top 20% SNPs with highest variant quality score after
892 having applied hard quality filtering as described for the VCF files in the BQSR procedure.

893 We used the produced VQSR recalibration files to filter the three candidate SNP VCFs with the Apply
894 Recalibration walker of the GATK setting the ‘--truth_sensitivity_filter_level’ to 99.8%. Finally, we
895 combined all SNPs of the three VCF files passing this filter using the *Combine Variants* tool of the
896 GATK, hence generating a master list of high-confidence SNP sites in the genus *Pongo*.

897 Step 3: We called the genotype of each study individual at the identified high-confidence SNP sites.
898 We performed genotyping on the recalibrated BAM files in multi-sample mode for Bornean and
899 Sumatran orangutans separately, producing one SNP VCF file per island.

900 Finally, we only retained positions with high genome mappability, *i.e.*, genomic positions within a
901 uniquely mappable 100-mers (up to 4 mismatches allowed), as identified with the GEM-mappability
902 module from the GEM library build [76]. This mappability mask excludes genomic regions in the
903 orangutan reference genome that are duplicated and therefore tend to produce ambiguous mappings,
904 which can lead to unreliable genotype calling. Furthermore, we aimed to reduce spurious male
905 heterozygous genotype calls on the X chromosome due to *UnifiedGenotyper* assuming diploidy of the
906 entire genome. We determined the male-to-female ratios (M/F) of mean observed heterozygosity (H_o)
907 and sequence coverage in non-overlapping 20-kb windows along the X chromosome across both
908 islands. We obtained a list of X-chromosomal windows where M/F of H_o was above the 85%-quantile
909 or M/F coverage was above the 95%-quantile, resulting in 1255 20-kb windows requiring exclusion.
910 We then repeated step 3 of the genotype calling pipeline on the X chromosome for the male samples
911 setting the argument ‘-ploidy’ of *UnifiedGenotyper* to 1 to specify the correct hemizygous state of the
912 X chromosome in males. We subsequently masked all X-chromosomal positions within the spurious
913 20-kb windows in both male and female samples.

914 In total, we discovered 30,640,634 SNPs among all 37 individuals, which represent the most
915 comprehensive catalogue of genetic diversity across the genus *Pongo* to date.

916 **QUANTIFICATION AND STATISTICAL ANALYSIS**

917 **Recombination map estimation**

918 We generated recombination maps for Bornean and Sumatran orangutans using the LDhat v2.2a
919 software [77], following Auton et al. [78]. We used a high-quality subset of genotype data from the
920 original SNP-calling dataset for the recombination map estimation for each island separately. Only
921 biallelic, non-missing and polymorphic SNPs were used. Filtered genotype data were split into
922 windows of 5,000 SNPs with an overlap of 100 SNPs at each side.

923 We ran the program *Interval* of the LDhat package for 60 million iterations, using a block penalty of
924 5, with the first 20 million iterations discarded as a burn-in. A sample was taken from the MCMC
925 chain every 40,000 iterations, and a point estimate of the recombination rate between each SNP was
926 obtained as the mean across samples. We joined the rate estimates for each window at the midpoint of

927 the overlapping regions and estimated *theta per site* for each window using the finite-site version of
 928 the Watterson's estimate, as described in Auton & McVean [77].

929 We tested the robustness of the method with regards to the observed genome-wide variation of *theta*
 930 by contrasting recombination rate estimates using window-specific and chromosomal-average *thetas*.
 931 *Thetas* twice as large that the genome average produced very similar $4N_e r$ (*rho*) estimates. Because of
 932 this, a single genome-wide average of *theta per site* was used for all the windows (Sumatra: $\theta_w =$
 933 0.001917 , Borneo: $\theta_w = 0.001309$). We then applied additional filters following Auton et al. [78]. SNP
 934 intervals larger than 50 kb, or *rho* estimates larger than 100, were set to zero and the 100 surrounding
 935 SNP intervals (-/+ 50 intervals) were set to zero recombination rate. A total of 1,000 SNP intervals
 936 were found to have $rho > 100$ for *P. abelii*, and 703 for *P. pygmaeus*. In addition, 32 gaps (> 50 kb)
 937 were identified for *P. abelii*, and 47 gaps for *P. pygmaeus*. After applying the +/- 50 interval criteria, a
 938 total of 7,424 SNP intervals were zeroed for *P. abelii*, and 15,694 for *P. pygmaeus*.

939 **Haplotype phasing**

940 We phased the genotype data from Bornean and Sumatran orangutans using a read aware statistical
 941 phasing approach implemented in SHAPEIT v2.0 [79, 80]. This allowed us to obtain good phasing
 942 accuracy despite our relatively low sample sizes by using phasing information contained in the
 943 pairedend sequencing reads to support the statistical phasing procedure. We used a high-quality subset
 944 of genotype data from the original SNP-calling dataset containing only biallelic and polymorphic
 945 SNPs. We first ran the program extractPIRs to extract phase informative reads (PIR) from the filtered
 946 BAM files. In a second step, we ran SHAPEIT in read aware phasing mode using the following
 947 parameters: 200 conditional states, 10 burnin iterations, 10 pruning iterations, 50 main iterations,
 948 and a window size of 0.5 Mb. Additionally, we provided two species-specific recombination maps
 949 (estimated with LDhat) and the PIR files obtained in the first step to the program.

950 SHAPEIT uses a recombination map expressed in cM/Mb, therefore it was necessary to convert the
 951 LDhat-based *rho* estimates to cM/Mb units ($rho=4N_e r$). Accordingly, we estimated island-specific
 952 effective population sizes using the Watterson's estimator of *theta* (Sumatra: $N_e[\theta_w]=41,000$, Borneo:
 953 $N_e[\theta_w]=27,000$) and applied these to the recombination map conversion. The most likely pair of
 954 haplotypes for each individual were retrieved from the haplotype graphs, and recoded into VCF file
 955 format.

956 **Individual heterozygosity and inbreeding**

957 We determined the extent of inbreeding for each individual by a genome-wide heterozygosity scan in
 958 sliding windows of 1 Mb, using a step size of 200 kb. We detected an excess of windows with very
 959 low heterozygosity in the density plots, pointing to some extent of recent inbreeding. To estimate the
 960 cutoff values of heterozygosity for the calculation of inbreeding coefficients, we calculated

961 heterozygosity thresholds for each island according to the 5th-percentile of the genome-wide
962 distribution of heterozygosities (Borneo: 1.0×10^{-4} heterozygote sites per bp; Sumatra: 1.3×10^{-4}).
963 Neighboring regions with heterozygosities below the cutoff value were merged to determine the
964 extent of runs of homozygosity (ROH). Based on the number and size of ROHs, we estimated the
965 percentage of the genome that is autozygous, which is a good measure of inbreeding [81]. We choose
966 1 Mb as window size for the calculation of heterozygosities based on previous studies identifying
967 regions smaller than 0.5 Mb as the result of background relatedness, and tracts larger than 1.6 Mb as
968 evidence of recent parental relatedness [82].

969 **Sex-specific genomic data: mitogenomes and Y chromosomes**

970 We produced complete mitochondrial genome (mitogenome) sequences for all study individuals. We
971 first created a consensus reference sequence from 13 Sanger-sequenced mitogenomes representing
972 almost all major genetic clusters of extant orangutans using BioEdit v7.2.0. [83]. The Sanger-
973 sequenced mitogenomes were generated via 19 PCRs with product sizes of 1.0–1.2 kb and an overlap
974 of 100–300 bp (Table S6) following described methods [84]. PCR conditions for all amplifications
975 were identical and comprised a pre-denaturation step at 94°C for 2 minutes, followed by 40 cycles
976 each with denaturation at 94°C for 1 minute, annealing at 52°C for 1 minute, and extension at 72°C
977 for 1.5 minutes. At the end, we added a final extension step at 72°C for 5 minutes. PCR products were
978 checked on 1% agarose gels, excised from the gel and after purification with the Qiagen Gel
979 Extraction Kit, sequenced on an ABI 3130xL sequencer using the BigDye Terminator Cycle
980 Sequencing kit (Applied Biosystems) in both directions using the amplification primers.

981 We individually mapped Illumina whole-genome sequencing reads of all 37 study individuals (Table
982 S4) to the consensus mitochondrial reference sequence using NovoAlign v3.02. (NovoCraft), which
983 can accurately handle reference sequences with ambiguous bases. This procedure prevented biased
984 short read mapping due to common population-specific mutations. For each individual, we generated
985 a FASTA sequence for the mitogenome with the *mpileup* pipeline of SAMtools. We only considered
986 bases with both mapping and base Phred quality scores ≥ 30 and required all positions to be covered
987 between 100 and 2000 times. Finally, we visually checked the sequence alignment of all individuals in
988 BioEdit and manually removed indels and poorly aligned positions and excluded the D-loop to
989 account for sequencing and alignment errors in those regions which might inflate estimates of mtDNA
990 diversity. In total, we identified 1,512 SNPs among all 50 individuals.

991 We thoroughly investigated the literature for the potential occurrence of nuclear insertions of mtDNA
992 (numts) in the genus *Pongo*, given that this has been a concern in closely related gorillas (*Gorilla*
993 spp.) [85]. There was no indication of numts in the genus *Pongo*, which is in line with our own
994 previous observations [28, 52, 53]. Numts also seem unlikely given our high minimal sequence depth
995 threshold.

996 We developed a comprehensive bioinformatics strategy to extract sequences from the male-specific
997 region of the Y chromosome (MSY) from whole-genome sequencing data. We expect the principle of
998 our bioinformatics strategy to be applicable to mammalian species in general if the taxon under
999 investigation is in phylogenetic proximity to one for which a Y-chromosomal reference sequence is
1000 present or will be made available. Like for most mammals, there is currently no reference Y
1001 chromosome for orangutans. Therefore, we had to rely on a reference assembly of a related species
1002 (*i.e.*, humans) for sequence read mapping. Despite the ~18 million years divergence between humans
1003 (*Homo* spp.) and orangutans [51, 86], we obtained a high number of MSY sequences. The impact of
1004 varying Y chromosome structure among species [87, 88] on sequence read mappability might have
1005 been reduced because we exclusively targeted X-degenerate regions. Hughes et al. [89] showed for
1006 human and chimpanzees that although less than 50% of ampliconic sequences have a homologous
1007 counterpart in the other species, over 90% of the X-degenerate sequences hold such a counterpart.

1008 We applied several filters to ensure male-specificity and single-copy status of the generated MSY
1009 sequences. (i) We simultaneously mapped sequencing reads to the whole orangutan reference genome
1010 *PonAbe2* [50] and not just the human reference Y chromosome, reducing spurious mapping of
1011 autosomal reads to the Y chromosome and allowing subsequent identification of reads that also
1012 aligned to the X or autosomal chromosomes. (ii) We exclusively accepted reads that mapped in a
1013 proper pair, *i.e.*, where both read mates mapped to the Y chromosome, which considerably increased
1014 confidence in Y-specific mapping. (iii) We also mapped whole-genome sequencing reads of 23
1015 orangutan females to the human Y reference chromosome and excluded all reference positions where
1016 female reads had mapped from the male Y sequence data. (iv) To exclude potential repetitive regions,
1017 we filtered nonuniquely mapped reads as well as positions with sequence coverage greater than two
1018 times the median coverage for each individual, as extensive coverage can be indicative for repetitive
1019 regions which might appear as collapsed regions on the Y reference chromosome. (v) To ensure that
1020 we only targeted unique, single-copy MSY regions, we exclusively retained reads mapping to four
1021 well-established X-degenerate regions of the MSY in humans [90].

1022 Our bioinformatics strategy consisted of the following detailed steps. First, we created a new reference
1023 sequence (*PonAbe2_humanY*) by manually adding the human reference Y chromosome (*GRCh37*) to
1024 the orangutan reference genome *PonAbe2* [50]. We then used BWA-MEM v0.7.5. [73] to map
1025 Illumina whole-genome short reads from 36 orangutans (13 males and 23 females) to this new
1026 reference sequence. We mapped reads for each individual separately in paired-end mode and with
1027 default settings. To reduce output file size, we removed unmapped reads on the fly using SAMtools
1028 v0.1.19 [91]. Picard v1.101 was used to add read groups and sort the BAM files. We then extracted all
1029 reads which mapped to the Y chromosome using SAMtools and marked read duplicates with Picard.

1030 We used the GATK [74, 75] to perform local realignment around indels and filtered out duplicated
1031 reads, bad read mates, reads with mapping quality zero and reads which mapped ambiguously. We

1032 called genotypes at all sequenced sites with the *Unified Genotyper* of the GATK, applying the output
1033 mode 'EMIT_ALL_CONFIDENT_SITES'. We called genotypes in multi-sample mode (females and
1034 males separately, sample-ploidy was set to 1), producing one genomic VCF file for each sex. We only
1035 accepted bases/reads for genotype calling if they had Phred quality scores ≥ 30 .

1036 From the VCF file of the females, we generated a 'nonspec' list with the coordinates of all sites with
1037 coverage in more than one female (minimal sequence depth $2x$), as these sites most likely were
1038 located in pseudoautosomal or ampliconic regions, *i.e.*, share similarity with the X or autosomal
1039 chromosomes. To ensure Y-specificity, we removed all sites of the 'nonspec' list from the VCF file of
1040 the males with VCFtools v0.1.12b. [92].

1041 Finally, we used GATK to extract sequences of four well-established X-degenerate regions of the
1042 MSY in humans (14,170,438–15,795,786; 16,470,614–17,686,473; 18,837,846–19,267,356;
1043 21,332,221–21,916,158 on the human reference Y chromosome assembly GRCh37/hg19)[90]. To be
1044 conservative, we chose regions which were longer than 1 Mb in humans and disregarded the first and
1045 last 300 kb of each region to account for potential uncertainties regarding region boundaries, leaving
1046 us with 3,854,654 bp in total. We exclusively retained genotype calls that were covered by a minimum
1047 of two reads and had a maximum of twice the individual mean coverage, resulting in 2,825,271 bp of
1048 MSY sequences among the 13 orangutan males. As expected, individual mean MSY sequence depth
1049 was about half (average: 54.4%) of that recorded for the autosomes, and ranged from 2.79–16.62x.
1050 For analyses, we only kept sites without missing data, *i.e.*, with a genotype in all study males. Because
1051 genomes of some individuals had been sequenced to only low coverage ($\sim 5\text{--}7x$) [50], this left us with
1052 673,165 bp of MSY sequences. We identified 1,317 SNPs among the 13 males, corresponding to a
1053 SNP density of 1 SNP every 511 bp.

1054 We constructed phylogenetic trees and estimated divergence dates for mitogenome and MSY
1055 sequences using the Bayesian Markov chain Monte Carlo (MCMC) method implemented in BEAST
1056 v1.8.0. [58]. To determine the most suitable nucleotide substitution model, we conducted model
1057 selection with jModelTest v2.1.4. [60]. Based on the Akaike information criterion (AIC) and corrected
1058 AIC, we selected the GTR+I substitution model [93] for mitogenomes and the TVM+I+G model [94]
1059 for MSY sequences.

1060 The mitogenome tree was rooted with a human and a central chimpanzee sequence from GenBank
1061 (accession numbers: GQ983109.1 and HN068590.1), the MSY tree with the human reference
1062 sequence *hg19*. We estimated divergence dates under a relaxed molecular clock model with
1063 uncorrelated lognormally distributed branch-specific substitution rates [95]. The prior distribution of
1064 node ages was generated under a birth-death speciation process [96]. We used fossil based divergence
1065 estimates to calibrate the molecular clock by defining a normal prior distribution for certain node
1066 ages. For mitogenomes, we applied two calibration points, *i.e.*, the *Pan-Homo* divergence with a mean
1067 age of 6.5 Ma and a standard deviation of 0.3 Ma [97, 98] and the Ponginae-Homininae divergence

1068 with a mean age of 18.3 Ma and a larger standard deviation of 3.0 Ma [86], which accounts for the
 1069 uncertainty in the divergence date [99]. For MSY sequences, we used the Ponginae-Homininae
 1070 divergence for calibration. We performed four independent BEAST runs for 30 million generations
 1071 each for mitogenomes, with parameter sampling every 1,000 generations, and for 200 million
 1072 generations each with parameter sampling every 2,000 generations for MSY sequences. We used
 1073 Tracer v1.6 [100] to examine run convergence, aiming for an effective sample size of at least 1000 for
 1074 all parameters. We discarded the first 20% of samples as burn-in and combined the remaining samples
 1075 of each run with LogCombiner v1.8.0. [58]. Maximum clade credibility trees were drawn with
 1076 TreeAnnotator v1.8.0.
 1077 [58] and trees visualized in FigTree v1.4.0. [101] and MEGA v6.06. [102].

1078 **Autosomal genetic diversity and population structure**

1079 For all subsequent population genetic analyses, we assumed an autosomal mutation rate (μ) of $1.5 \times$
 1080 10^8 per base pair per generation, based on estimates obtained for the present-day mutation rates in
 1081 humans and chimpanzees, derived primarily from de novo sequencing comparisons of parent-
 1082 offspring trios but also other evidence [103-106]. There is good reason to believe that the mutation
 1083 rate in orangutans is similar to that in other great apes, given the very similar branch lengths from
 1084 outgroups such as gibbon and macaque to each species [107]. We assumed a generation time of 25
 1085 years [108].

1086 We identified patterns of population structure in the autosomal genome by principal component
 1087 analysis

1088 (PCA) of biallelic SNPs using the function ‘prcomp’ in R v3.2.2 [109]. Three separate analyses were
 1089 performed: one within each island and one including all study individuals. For each sample set, we
 1090 excluded all genotypes from the SNP VCF files that were covered by less than five reads and only
 1091 retained SNPs with a genotype call in all individuals after this filter. Furthermore, we removed SNPs
 1092 with more than two alleles and monomorphic SNPs in the particular sample set. This restrictive
 1093 filtering left us with 3,006,895 SNPs for the analysis of all study individuals, 5,838,796 SNPs for PCA
 1094 within Bornean orangutans and 4,808,077 SNPs for PCA within Sumatran orangutans.

1095 We inferred individual ancestries of orangutans using ADMIXTURE v1.23 [110]. We randomly
 1096 sampled one million sites from the original VCF files and filtered this subset by excluding sites with
 1097 missing genotypes or with a minor allele frequency less than 0.05. We further reduced the number of
 1098 sites to 272,907 by applying a linkage disequilibrium (LD) pruning filter using PLINK v1.90b3q (`-`
 1099 `indep_pairwise 50 5 0.5`) [111]. ADMIXTURE was run 20 times at all K values between 1 and 10.
 1100 Among those runs with a difference to the lowest observed cross validation (CV) error of less than 0.1
 1101 units, we reported the replicate with the highest biological meaning, *i.e.*, runs that resolved
 1102 substructure among different sampling areas rather than identifying clusters within sampling areas.

1103 For subsequent analyses, we defined seven distinct populations based on the results of the PCA and
1104 ADMIXTURE analyses: three on Sumatra (Northeast Alas comprising North Aceh and Langkat
1105 regions, West Alas, and Batang Toru) and four on Borneo (East Kalimantan, Sarawak, Kinabatangan
1106 comprising North and South Kinabatangan, and Central/West Kalimantan comprising Central and
1107 West Kalimantan). Even though individuals from North and South Kinabatangan could be clearly
1108 distinguished in the PCA and ADMIXTURE analysis, we decided to pool the two Kinabatangan
1109 populations due to their low samples sizes ($n = 2$). This can be justified as data from the mitochondrial
1110 genome showed that they started to diverge only recently (~40 ka).

1111 **Ancestral gene flow between orangutan populations**

1112 We used D-statistics to assess gene flow between orangutan species, testing all three possible
1113 phylogenetic relationships among *P. abelii*, *P. tapanuliensis*, and *P. pygmaeus*. We extracted
1114 genotype data from the two individuals per population with the highest sequencing coverage and
1115 included two human genome sequences as outgroup (SRA sample accession: ERS007255 and
1116 ERS007266). We calculated D-statistics for all combinations of populations involving the three
1117 species using the qpDstat program of the ADMIXTOOLS package v4.1 and assessed significance
1118 using the block jackknife procedure implemented in ADMIXTOOLS.

1119 To explore temporal patterns of gene flow between orangutan populations, we applied the multiple
1120 sequential Markovian coalescent (MSMC2) model [112]. The rate of coalescence of
1121 between-population haplotype pairs was compared to the within-population coalescence rate of
1122 haplotype pairs from the same population to obtain the relative cross-coalescence rate (RCCR)
1123 through time. A RCCR close to 1 indicates extensive gene flow between populations, while a ratio
1124 close to 0 indicates complete genetic isolation.

1125 We used the phased whole-genome data for the relative cross-coalescence rate analysis. To avoid
1126 coverage-related issues, we selected the individual with the highest sequencing coverage for each
1127 population. We further excluded sites with an individual sequencing coverage less than 5x, a mean
1128 mapping quality less than 20, or sites with low mappability based on the mappability mask.

1129 We ran MSMC2 for all pairs of populations, using a single individual (*i.e.*, two haplotypes) per
1130 population. For each population pair, we performed three individual MSMC2 runs, using the default
1131 time discretization parameters: within population 1 (two haplotypes; -I 0,1), within population 2 (two
1132 haplotypes; -I 2,3), and between populations (four haplotypes; -I 0,1,2,3 -P 0,0,1,1). We then used the
1133 combineCrossCoal.py Python script of the MSMC2 package to combine the outputs of the three runs
1134 into a combined output file.

1135 As the sequencing coverage of the best Batang Toru individual was substantially lower compared to
1136 individuals from other populations (~17x vs. ~23–27x, Table S4), we also assessed whether different
1137 sequencing coverage was negatively affecting the relative cross-coalescence rate results. To achieve

1138 this, we repeated the analysis using individuals with similar coverage as the Batang Toru individual
1139 (~16–21x). The results were highly consistent with the output from the runs with the highest-coverage
1140 individuals, indicating that the relative cross-coalescent rate analysis was robust to differences in
1141 sequencing coverage in our data set.

1142 **Approximate Bayesian Computation (ABC)**

1143 To gain insights into the colonization history of the Sundaland region by orangutans and obtain
1144 parameter estimates of key aspects of their demographic history, we applied a model-based ABC
1145 framework [31]. For this, we sampled a total of 3,000 independent sequence loci of 2 kb each,
1146 following the recommendations in Robinson et al. [113]. Loci were sampled randomly from non-
1147 coding regions of the genome, with a minimum distance of 50 kb between loci to minimize the effects
1148 of linkage. Since the coalescent simulations underlying ABC inference assume neutrality, we
1149 excluded loci located within 10 kb of any exonic region defined in the *Pongo abelii* Ensembl gene
1150 annotation release 78, as well as loci on the X chromosome and the mitochondrial genome, which
1151 would exhibit reduced N_e as compared to the autosomal regions.

1152 For all ABC-based modelling, we defined three metapopulations for the calculation of summary
1153 statistics: Sumatran populations north of Lake Toba (NT), the Sumatran population of Batang Toru
1154 south of Lake Toba (ST), as well as all Bornean populations (BO). For each metapopulation as well as
1155 over all metapopulations combined, we calculated the first four moments over all loci for the
1156 following summary statistics: nucleotide diversity (π), Watterson's theta, and Tajima's D.
1157 Furthermore, for each of the three pairwise comparisons between metapopulations, we calculated the
1158 first four moments over loci of the number of segregating sites, proportions of shared and fixed
1159 polymorphism, average sequence divergence (d_{XY}), and Φ_{ST} [114]. To avoid potential problems with
1160 unreliable phasing, we only used summary statistics that do not require phased sequence data. This
1161 resulted in a total of 108 summary statistics used in the ABC analyses. For each locus, we extracted
1162 genotype data of a total of 22 individuals (5 Northeast Alas, 5 West Alas, 2 Batang Toru, 4
1163 Central/West Kalimantan, 2 East Kalimantan, 2 Sarawak, 2 Kinabatangan) by selecting the
1164 individuals with the highest sequence coverage for a given locus. Additionally, we recorded the
1165 positions of missing data for each locus and individual and coded genotypes as 'missing' in the
1166 simulated data if mutations fell within the range of missing data in the observed data.

1167 In a first step, we used a model testing framework to infer the most likely sequence of population
1168 splits in the colonization history of orangutans. For this, we designed four models representing
1169 potential colonization patterns into Sundaland (Figure 3A). We assumed a simplified population
1170 structure with three distinct, random mating units composed of NT, ST, and BO metapopulations as
1171 described above. We simulated 4×10^6 data sets for each model using the coalescent simulator ms
1172 [115]. Since we obtained a large number of summary statistics, we used a partial least squares

1173 discriminant analysis (PLS-DA) to extract the orthogonal components of the summary statistics that
1174 are most informative to discriminate between the four competing models using the ‘plsda’ function of
1175 the R package ‘mixOmics’ v5.2.0 [116] in R version 3.2.2 [109]. For model testing, we used the R
1176 package ‘abc’ v2.1 [117] to perform a multinomial logistic regression on the PLS transformed
1177 simulated and observed summary statistics, using a tolerance level of 0.05% (8,000 simulations
1178 closest to the observed data). To find the optimal number of PLS components for model selection, we
1179 performed cross-validations with 200 randomly chosen sets of summary statistics for each model and
1180 assessed model misspecification rates when using 10, 12, 15, 18, and 20 components.

1181 We found that using the first 18 PLS components resulted in the lowest model misspecification rate.
1182 However, our model testing approach lacked power to reliably differentiate between pairs of models
1183 with the same underlying species tree (*i.e.*, model 1a vs. model 1b and model 2a vs. model 2b in
1184 Figure 3A), as evidenced by a high model misspecification rate of 47.63% across all four models. In
1185 order to increase discrimination power with a new set of optimized PLS components, we therefore
1186 repeated the PLS-DA and multinomial logistic regression with the two best-fitting models (model 1a
1187 vs. model 1b). This resulted in a substantially lower model misspecification rate (36.00%). Moreover,
1188 no model misassignment occurred with a posterior probability equal or higher than the observed value
1189 (0.976), indicating a high confidence in the selected model (model 1a).

1190 After establishing the order of population split events, we were interested in parameter estimates of
1191 different aspects of the orangutan demographic history. For this, we applied a more complex model
1192 that included additional population structure in NT and BO, as well as recent population size changes
1193 (Figure 3B). The design of this model was informed by (i) PCA and ADMIXTURE analyses (Figs. 2B
1194 and 2C), (ii) MSMC2 analyses (Figure 3C), and (iii) previous demographic modeling using more
1195 limited sets of genetic markers [57]. For parameter estimation, we performed a total of 1×10^8
1196 simulations as described above. Model parameterization and parameter prior distributions are shown
1197 in Table S5. We used 100,000 random simulations to extract the orthogonal components of the
1198 summary statistics that maximize the covariance matrix between summary statistics and model
1199 parameters using the ‘plsr’ function of the R package ‘pls’ v2.5-0 [118]. We defined the optimal
1200 number of partial least squares (PLS) components based on the drop in the root mean squared error for
1201 each parameter with the inclusion of additional PLS components [119]. After transforming both the
1202 simulated and observed summary statistics with the loadings of the extracted PLS components, we
1203 performed ABC-GLM postsampling regression [120] on the simulations with the smallest Euclidean
1204 distance to the observed summary statistics using ABCtoolbox v2.0 [121]. To find the optimal
1205 proportion of retained simulations, we assessed the root-mean-integrated-squared error of the
1206 parameter posterior distributions based on 1,000 pseudo-observed data sets (pods) randomly chosen
1207 from the simulated data. We found that varying the tolerance level had little impact on the accuracy of

1208 the posterior distributions and therefore used a tolerance level of 0.00002 (equaling 2,000 simulations)
1209 for parameter estimation.

1210 To assess the goodness of fit of our demographic model, we calculated the marginal density and the
1211 probability of the observed data under the general linear model (GLM) used for the post-sampling
1212 regression with ABCtoolbox [120]. A low probability of the observed data under the GLM indicates
1213 that the observed data is unlikely to have been generated under the inferred GLM, implying a bad
1214 model fit. We obtained a p-value of 0.14, showing that our complex demographic model is well able
1215 to reproduce the observed data. Additionally, we visualized the coverage of summary statistics
1216 generated under the demographic model relative to the observed data by plotting the first 12 principal
1217 components of the simulated and observed data. For this, we randomly selected 100,000 simulations
1218 and extracted

1219 PCA components using the ‘prcomp’ function in R. The observed data fell well within the range of
1220 simulated summary statistics for all 12 components. Furthermore, we checked for biased posterior
1221 distributions by producing 1,000 pods with parameter values drawn from the prior distributions. For
1222 each pods, we determined the quantile of the estimated posterior distribution within which the true
1223 parameter values fell and used a Kolmogorov-Smirnov in R to test the resulting distribution of
1224 posterior quantiles for uniformity. Deviations from uniformity indicate biased posterior distributions
1225 [122] and the corresponding parameter estimates should be treated with caution. As expected from
1226 complex demographic models, multiple parameters showed significant deviations from uniformity
1227 after sequential Bonferroni correction [123]. However, in most of these distributions, data points were
1228 overrepresented in the center of the histogram, which indicates that posterior distributions were
1229 estimated too conservatively.

1230 **G-PhoCS analysis**

1231 We used the full-likelihood approach implemented in G-PhoCS v1.2.3 [124] to compare different
1232 models of population splitting with gene flow and to estimate parameters of the best-fitting model.
1233 Due to computational constraints, we limited our data set to eight individuals with good geographic
1234 coverage of the extant orangutan distribution (1 Northeast Alas, 1 West Alas, 2 Batang Toru, 2
1235 Central/West Kalimantan, 1 East Kalimantan, 1 Kinabatangan). We sampled 1-kb loci across the
1236 autosomal genome, ensuring a minimum distance of 50 kb among loci to minimize linkage. To reduce
1237 the impact of natural selection, we excluded loci located within 1 kb of any exonic region defined in
1238 the *Pongo abelii* Ensembl gene annotation release 78. We coded sites as missing based on the
1239 following filter criteria: low mappability, mean mapping quality less than 20, and individual coverage
1240 less than 5x. Sites without at least one valid genotype per species were excluded completely. We only
1241 retained loci with at least 700 bp of sites with data, resulting in a total of 23,380 loci for which we
1242 extracted genotype information for the eight selected individuals.

1243 We compared models with the three different possible underlying population trees in a three taxon
 1244 setting (Borneo, Sumatra north of Lake Toba, and Batang Toru). We performed 16 independent
 1245 GPhoCS runs for each model, running the MCMC algorithm for 300,000 iterations, discarding the
 1246 first 100,000 iterations as burn-in and sampling every 11th iteration thereafter. The first 10,000
 1247 iterations were used to automatically adjust the MCMC finetune parameters, aiming for an acceptance
 1248 rate of the MCMC algorithm of 30–40%. We merged the resulting output files of independent runs
 1249 and analysed them with Tracer v1.6 [100] to ensure convergence among runs. We then used the model
 1250 comparison based on the Akaike information criterion through MCMC (AICM) [125, 126]
 1251 implemented in Tracer to assess the relative fit of the three competing models.

1252 In agreement with the ABC analyses, the model positing the deepest split between Sumatra north of
 1253 Lake Toba and Batang Toru, followed by a split between south of Lake Toba and Borneo, showed a
 1254 much better fit to the data compared to the two other splitting patterns. Independent replicates of the
 1255 same model produced highly consistent posterior distributions, indicating convergence of the MCMC
 1256 algorithm. All parameters of the best-fitting model were estimated with high precision, as shown by
 1257 the small 95%-highest posterior density ranges (Table S5). Compared to the estimates from the ABC
 1258 analysis, G-PhoCS resulted in more recent divergence time estimates for both the NT/(BO,ST) and
 1259 BO/ST splits. This discrepancy might be caused by hypermutable CpG sites, which likely violate
 1260 certain assumptions of the G-PhoCS model [124]. We could not exclude CpG sites in our analysis due
 1261 to the absence of a suitable outgroup for calibration. Instead, we had to rely on a fixed genome-wide
 1262 mutation rate, which includes hypervariable CpG sites. An alternative explanation could be a likely
 1263 bias in the G-PhoCS results due to the restriction to a highly simplified demographic model as
 1264 compared to our ABC analyses; G-PhoCS assumes constant effective population sizes and migration
 1265 rates in between population splits. However, this assumption is most likely violated in orangutans, as
 1266 shown by the results of our ABC analysis (Figure 3B, Table S5).

1267 **Cranial, dental, and mandibular morphology**

1268 We evaluated five qualitative and 44 quantitative cranial, dental, and mandibular variables (Tables S1
 1269 and S2). We chose variables that had previously been used to describe and differentiate orangutan
 1270 cranio-mandibular shape [61-63, 127-132]. Due to extensive dental wear of the Batang Toru
 1271 specimen, we limited our comparisons with the Padang cave material to the breadth of the upper and
 1272 lower canines, in addition to the length, breadth, and area (*i.e.*, breadth x length) of the lower first
 1273 molar, all of which displayed a limited amount of wear. All measurements were taken by a single
 1274 individual (AnN) in order to reduce observer bias.

1275 We used both univariate and multivariate statistics to evaluate the Batang Toru specimen in relation to
 1276 our comparative sample. As Batang Toru is only represented by a single sample, we first compared it
 1277 to the interquartile range (IQR, defined as the range between the first and the third quartile) and the

1278 lower and upper inner fence ($\pm 1.5 \times \text{IQR}$) for each separate sample population, using traditional
1279 methods for evaluating outliers [133]. This allowed us to evaluate the Batang Toru specimen's
1280 distance and direction from the central tendency of our sample orangutan populations. We also
1281 conducted univariate exact permutation tests for each morphological variable by removing a single
1282 sample for either the *P. abelii*, *P. pygmaeus*, or *P. p. palaeosumatrensis* sample populations and then
1283 comparing the linear distance to the mean of the remaining samples. This was done for each sample
1284 until all samples had a calculated value. A linear distance between the *P. tapanuliensis* sample and the
1285 *P. abelii*, *P. pygmaeus*, and *P. p. palaeosumatrensis* mean values (*i.e.*, the test statistics) was then
1286 calculated and compared to the sample distributions detailed above. P-values represent the number of
1287 samples from the sample distribution that exceed the test statistic, divided by the total number of
1288 comparisons. In some cases, specimens did not preserve the measurements utilized in this study (*e.g.*,
1289 broken bone elements and/or missing/heavily worn teeth), and so were excluded from comparisons.
1290 Sample sizes for univariate comparisons of extant orangutan cranio-mandibular morphology are
1291 detailed in Table S1, whereas the sample sizes for the univariate comparisons of extant and fossil teeth
1292 are detailed in Table S2.

1293 We also conducted a PCA on 26 of our 39 cranio-mandibular variables, on a subset of our extant
1294 orangutan sample, including *P. abelii* (n=8), *P. pygmaeus* (n=19), and the newly described *P.*
1295 *tapanuliensis* specimen. The choice of 26 variables allowed us to maximize sample size and avoid
1296 violating the assumptions of PCA [134]. A scree plot (using the *princomp* function from the base *stats*
1297 package in R [135]) indicated that seven principal components were sufficient to be extracted, based
1298 on the Kaiser criterion of eigenvalues at ≥ 1 [136]. Using the *principal* function from the *psych* R
1299 package [137], we ran a PCA on the correlation matrix of our 26 selected variables, extracting seven
1300 principal components with varimax rotation.

1301 To highlight the multivariate uniqueness of *P. tapanuliensis*, we used the extracted PCs and calculated
1302 the Euclidean D^2 distance for each sample relative to the *P. abelii* and *P. pygmaeus* centroids. We
1303 grouped these distances into two distributions, referred to as the between species (*i.e.*, the distances of
1304 all *P. abelii* samples to the *P. pygmaeus* centroid plus all of the *P. pygmaeus* samples to the *P. abelii*
1305 centroid) and within species (*i.e.*, the distances of all *P. abelii* samples to the *P. abelii* centroid plus all
1306 of the *P. pygmaeus* samples to the *P. pygmaeus* centroid) distributions. We then compared the
1307 Euclidean D^2 distances of *P. tapanuliensis* to the *P. abelii* and *P. pygmaeus* centroids (*i.e.*, the test
1308 values), relative to the two aforementioned sample distributions. Exact permutation p-values for these
1309 results were calculated as the number of samples from the sample distribution that exceed the test
1310 statistic, divided by the total number of comparisons. All Euclidean D^2 distance were calculated in the
1311 base *stats* package in R [135].

1312 **Acoustic and behavioral analyses**

1313 We used both previously published [138-140] and newly collected data in our analyses of male long
1314 calls. The current study includes $n=130$ calls from $n=45$ adult males across 13 orangutan field sites. In
1315 addition to two individuals from Batang Toru, we sampled 14 individuals of *P. abelii* and 29
1316 individuals of *P. pygmaeus*. Using our comparative sample, we evaluated 15 long call variables (Table
1317 S3). We chose variables and their definitions that had previously been described to differentiate
1318 orangutan male long calls [138, 139, 141].

1319 We used both univariate and multivariate statistics to evaluate the Batang Toru specimen in relation to
1320 our comparative sample. As Batang Toru is only represented by two individuals, we compared the
1321 mean of these two sample points to the interquartile range (IQR) and the lower and upper inner fence
1322 ($\pm 1.5 \cdot \text{IQR}$) for each separate sample population [133]. As above, univariate exact permutation tests
1323 were conducted for each long call variable by removing a single sample for either the *P. abelii* or *P.*
1324 *pygmaeus* sample populations and then comparing the linear distance to the mean of the remaining
1325 samples. This was done for each sample until all samples had a calculated value. A linear distance
1326 between the average of the two *P. tapanuliensis* samples and the *P. abelii* or *P. pygmaeus* mean
1327 values (*i.e.*, the test statistics) was then calculated and compared to the sample distributions detailed
1328 above. P-values represent the number of samples from the sample distribution that exceed the test
1329 statistic, divided by the total number of comparisons. In some cases, not all acoustic variables were
1330 available for each individual. As such, sample sizes for univariate comparisons are detailed in Table
1331 S3.

1332

1333 **Geological and ecological analyses**

1334 We evaluated five ecological variables, including the type and age of geological parent material,
1335 elevation, average temperature, and average rainfall, to highlight that the current ecological niche of
1336 *P. tapanuliensis* is divergent relative to that of *P. abelii* and *P. pygmaeus*. For Sumatran populations,
1337 type and age of geological parent material were digitized from the land unit and soil map series of
1338 Sumatra [142-149]. No comparable geospatial data is available for Borneo, so we used previously
1339 published materials to more broadly characterize areas populated by orangutans [150]. To maintain
1340 consistency, elevation, average temperature, and average annual rainfall were collected from the
1341 WorldClim v. 1.4 bioclimatic variables dataset [151]. Using the digitized land unit/soil maps, we
1342 calculated the percentage of Sumatran orangutan distribution [152] classified into four classes for each
1343 type (*e.g.*, igneous, metamorphic, sedimentary, and other rock [*i.e.*, land units with a mixture of rock
1344 types]) and age (*e.g.*, Pre-Cenozoic, Tertiary, Quaternary, and other [*i.e.*, land units with a mixture of
1345 ages]) of geological parent material. For the elevation and climatic variables, we created 1km x 1km

1346 sample point grids for each currently identified orangutan population in Borneo and Sumatra [152,
1347 153], and sampled the three aforementioned WorldClim datasets.

1348 **DATA AND SOFTWARE AVAILABILITY**

1349 Raw sequence read data have been deposited into the European Nucleotide Archive (ENA;
1350 <http://www.ebi.ac.uk/ena>) under study accession number PRJEB19688. Mitochondrial and
1351 Ychromosomal sequences are available from the Mendeley Data repository under ID code
1352 doi:10.17632/hv2r94yz5n.1.

KEY RESOURCES TABLE

REAGENT or RESOURCE	SOURCE	IDENTIFIER
Biological Samples		
17 <i>Pongo</i> spp. whole blood samples	This paper	See Table S4
34 <i>Pongo</i> spp. cranial specimens	This paper	N/A
Chemicals, Peptides, and Recombinant Proteins		
Proteinase K (20 mg/ml)	Promega	Cat#V3021
Critical Commercial Assays		
Genra Puregene Blood Kit	Qiagen	Cat#158467
Deposited Data		
<i>Pongo abelii</i> reference genome <i>ponAbe2</i>	[50]	http://genome.wustl.edu/genomes/detail/pongo-abelii/
<i>Pongo abelii</i> Ensembl gene annotation release 78	Ensembl	https://www.ensembl.org/Pongo_abelii/Info/Index
Human reference genome NCBI build 37, GRCh37	Genome Reference Consortium	http://www.ncbi.nlm.nih.gov/projects/genome/assembly/grc/human/
Whole-genome sequencing data of 5 <i>Pongo abelii</i>	[50]	SRA: PRJNA20869
Whole-genome sequencing data of 5 <i>Pongo pygmaeus</i>	[50]	SRA: PRJNA74653
Whole-genome sequencing data of 10 <i>Pongo</i> spp.	[51]	SRA: PRJNA189439
Whole-genome sequencing data of 17 <i>Pongo</i> spp.	This paper	ENA: PRJEB19688
Whole-genome sequencing data of 2 <i>Homo sapiens</i>	Human Genome Diversity Project	SRA: ERS007255 and ERS007266
13 <i>Pongo</i> MSY sequences	This paper	http://dx.doi.org/10.17632/hv2r94yz5n.1
50 <i>Pongo</i> mitochondrial genome sequences	This paper	http://dx.doi.org/10.17632/hv2r94yz5n.1
Pictures of paratypes	This paper	https://morphobank.org/index.php/Projects/ProjectOverview/project_id/2591
Additional supporting information and analyses	This paper	https://morphobank.org/index.php/Projects/ProjectOverview/project_id/2591
Oligonucleotides		
19 mitochondrial primer pairs	This paper	See Table S6

Software and Algorithms		
FastQC v0.10.1.	[72]	https://www.bioinformatics.babraham.ac.uk/projects/fastqc/
BWA v0.7.5	[73]	http://bio-bwa.sourceforge.net/
Picard Tools v1.101		http://broadinstitute.github.io/picard/

GATK v3.2.2.	[74, 75]	https://software.broadinstitute.org/gatk/
GEM library	[76]	http://algorithms.wtf/gem-library
LDhat v2.2a	[77]	https://github.com/auton1/LDhat
SHAPEIT v2.0	[79]	https://mathgen.stats.ox.ac.uk/genetics_software/shapeit/shapeit.html
BioEdit v7.2.0.	[154]	http://www.mbio.ncsu.edu/bioedit/page2.html
NovoAlign v3.02.	Novocraft	http://www.novocraft.com/products/novoalign/
SAMtools v0.1.19	[155]	http://www.htslib.org/
VCFtools v0.1.12b.	[156]	https://vcftools.github.io/index.html
BEAST v1.8.0.	[58]	http://beast.community/index.html
jModelTest v2.1.4.	[60]	https://github.com/ddarriba/jmodeltest2
Tracer v1.6		http://tree.bio.ed.ac.uk/software/tracer/
FigTree v1.4.0.		http://tree.bio.ed.ac.uk/software/figtree/
MEGA v6.06.	[102]	http://www.megasoftware.net/mega.php
R 3.2.2	[109]	https://www.rproject.org
ADMIXTURE v1.23	[110]	https://www.genetics.ucla.edu/software/admixture/index.html
PLINK v1.90b3q	[111]	https://www.coggenomics.org/plink2
ADMIXTOOLS v4.1	[157]	https://github.com/DReichLab/AdmixTools

MSMC2	[112]	https://github.com/stschiff/msmc2
ms	[115]	http://home.uchicago.edu/rhudson1/source/mksamples.html
R package 'mixOmics' v5.2.0	[116]	https://www.rdocumentation.org/packages/mixOmics
R package 'abc' v2.1	[117]	https://cran.rproject.org/package=abc
R package 'pls' v2.5-0	[118]	https://cran.rproject.org/package=pls

ABCtoolbox v2.0	[121]	http://www.unifr.ch/biology/research/wegmann/wegmannsoft
G-PhoCS v1.2.3	[124]	http://compgen.cshl.edu/GPhoCS/
R package 'psych'	[137]	https://cran.rproject.org/package=psych
R package 'MASS'	[158]	https://cran.rproject.org/package=MASS

Figure 1

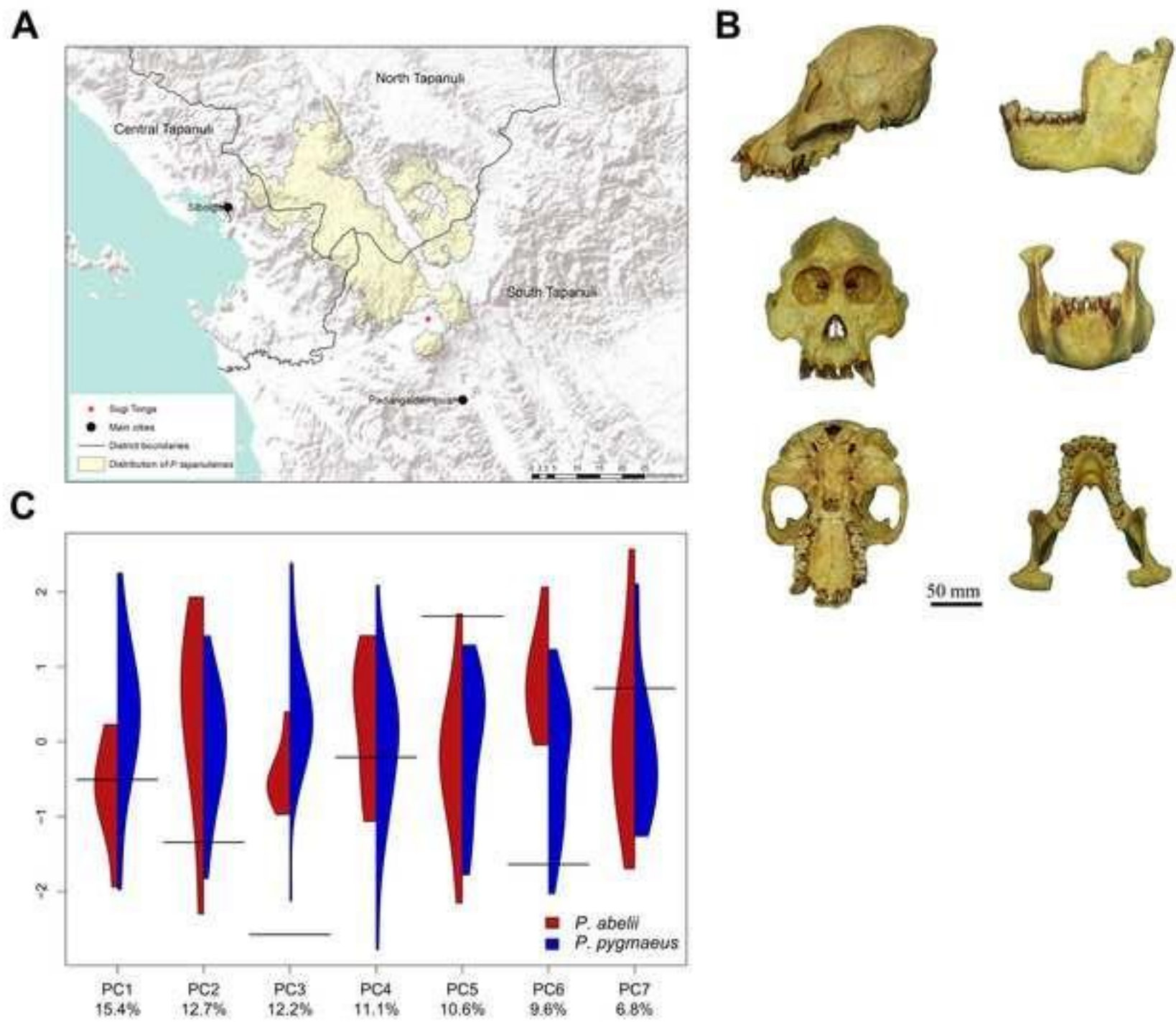


Figure 2

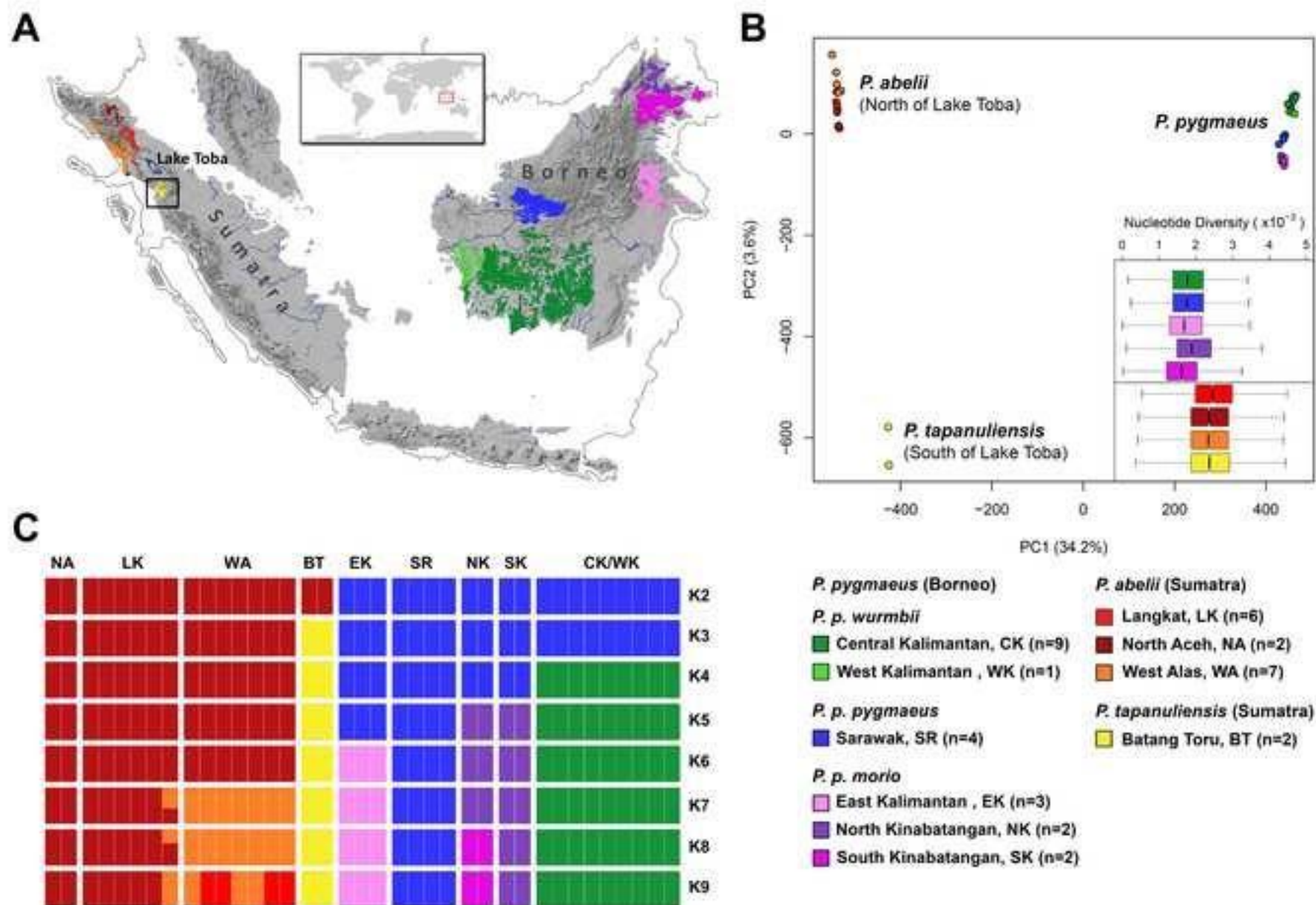
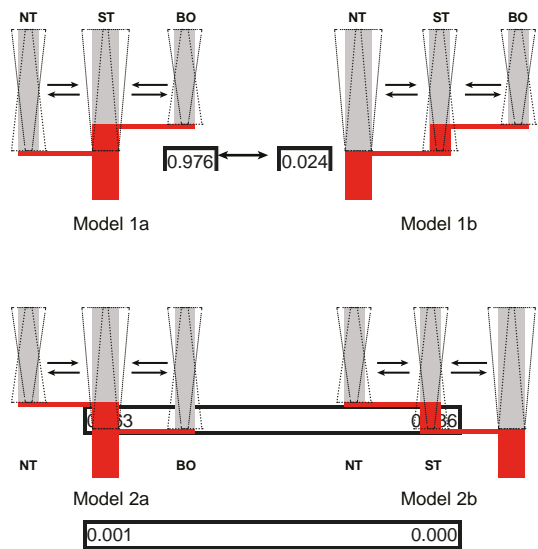
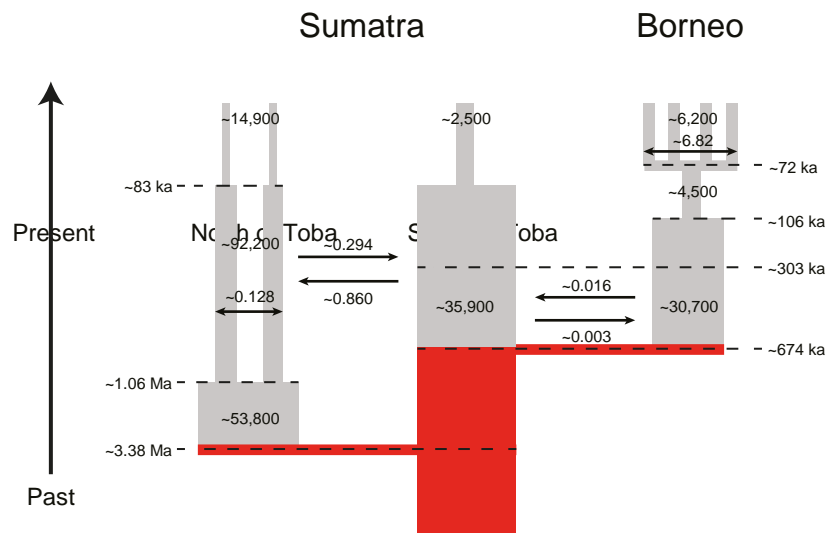


Figure 3

A



B



C

Figure 4

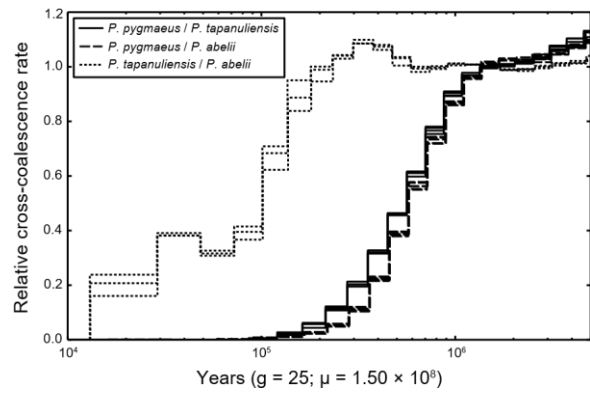
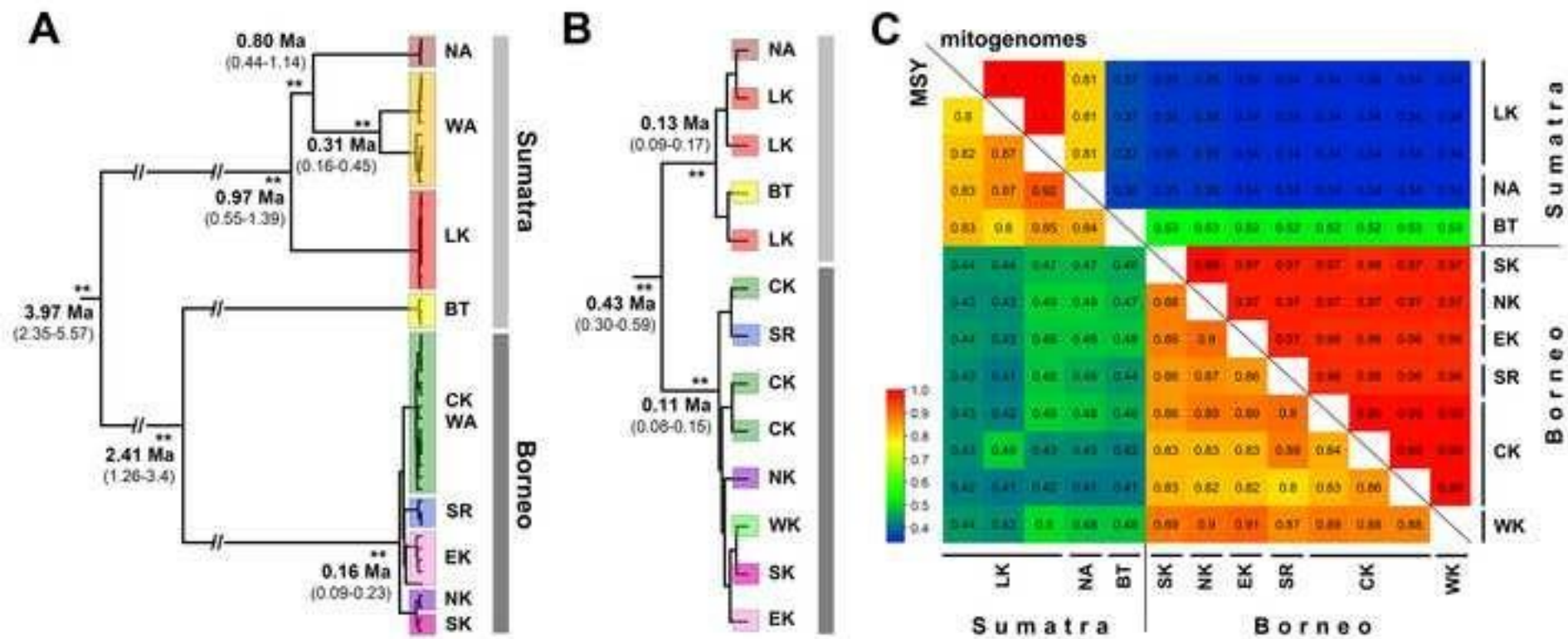


Figure 5



Supplemental References

- S1. Locke, D.P., Hillier, L.W., Warren, W.C., Worley, K.C., Nazareth, L.V., Muzny, D.M., Yang, S.-P., Wang, Z., Chinwalla, A.T., Minx, P., et al. (2011). Comparative and demographic analysis of orang-utan genomes. *Nature* 469, 529-533.
- S2. Prado-Martinez, J., Sudmant, P.H., Kidd, J.M., Li, H., Kelley, J.L., Lorente-Galdos, B., Veeramah, K.R., Woerner, A.E., O'Connor, T.D., Santpere, G., et al. (2013). Great ape genetic diversity and population history. *Nature* 499, 471-475.